1-1-2009

Microemulsion-Based Solid Lipid Nanoparticles As Emulsion Stabilisers

Elham H. Hazfi
Ryerson University

MICROEMULSION-BASED SOLID LIPID NANOPARTICLES AS EMULSION STABILISERS

by

Elham Hassanzadeh Hazfi
Bachelor of Science, Shaheed Beheshti University, Tehran, Iran, 1993

A thesis
presented to Ryerson University
in partial fulfillment of the
requirements for the degree of
Master of Science
in the Program of
Molecular Science

Toronto, Ontario, Canada, 2009

I hereby declare that I am the sole author of this thesis or dissertation.
I authorize Ryerson University to lend this thesis or dissertation to other institutions or individuals for the purpose of scholarly research.

---

* Signature

I further authorize Ryerson University to reproduce this thesis or dissertation by photocopying or by other means, in total or in part, at the request of other institutions or individuals for the purpose of scholarly research.

---

*Signature

MICROEMULSION-BASED SOLID LIPID NANOPARTICLES AS EMULSION STABILISERS

©Elham Hassanzadeh Hazfi

Master of Science, Department of Chemistry and Biology
Ryerson University, Toronto, Canada, 2009

Abstract

The preparation and properties of water-in-oil (W/O) emulsions stabilised solely by adsorbed surface-active solid lipid nanoparticles (SLNs) at the oil-water interface were studied.

Monostearin-based SLNs were prepared using food-grade microemulsions as nanoscale 'reactors'. Hot oil-in-water (O/W) microemulsions (70 °C) consisting of monostearin, Tween 20, ethanol and water were crash-cooled to 4 °C to promote the liquid-solid transition of the monostearin and thus develop sub-micron solid lipid particles.

SLNs obtained from the cooled microemulsions were partially stabilised with addition of lecithin (0.5% w/w) to the microemulsion system. With 2% (w/w) added monostearin, the W/O emulsion was stable for the 14 days of study. The microstructure of the emulsions revealed the presence of two stabilisation mechanisms, namely Pickering-type and continuous phase crystal network stabilisation, which both contributed to slowing dispersed droplet coalescence.

Overall, this study demonstrated that surface-active SLNs developed using a microemulsion technique could effectively kinetically stabilise model W/O emulsions.

Acknowledgements

First and foremost, I would like to thank my supervisor, Dr. Dérick Rousseau, who shared with me much of his expertise and research insight. With his enthusiasm, patience and his great efforts to explain things clearly and simply, he helped me through each step of this research. Throughout my thesis-writing period, he provided encouragement and sound advice to help me work to the best of my ability. I would also like to express my gratitude to Drs. Darrick Heyd and Christopher Evans, my committee members, whose thoughtful advice often served to give me a further sense of direction during my Masters studies.

I wish to thank everybody with whom I have shared experiences in life. From the people who first persuaded and got me interested into continuing my education, especially those who also played a significant role in my life, to those whose company made my days more enjoyable. I must individually thank all of my friends and members of the lab 'crew', especially Dr. Supratim Ghosh, Shane Hodge, Afra Pourdad, Roomana Aafaqi and Muhammad Naqvi.

I cannot finish without saying how grateful I am to my family. Particular thanks go to my dear husband, Farzad and my beloved daughter, Shauli. Lastly, and most importantly, I wish to thank my mother, Fatemeh Asri and my sister Mahssa Hazfi who always supported me. Without their help, this work would not have been possible. To them I dedicate this thesis.

Table of contents

List of tables

List of figures

Chapter 1

Introduction

Colloids comprise a broad class of materials whose basic structure consists of a dispersion of one phase in another [1]. Some colloids are thermodynamically stable and generally form spontaneously, such as microemulsions in which two immiscible fluids are stabilised by the presence of an amphiphilic molecule (surfactant) and a co-surfactant, usually an alcohol. Metastable colloids, *e.g.*, emulsions, require energy for preparation. They generally consist of two immiscible fluids, usually water and oil, with one fluid dispersed in the other, and are stabilised by the presence of surface-active agents [1-3]. A system that consists of oil droplets dispersed in an aqueous phase is called an oil-in-water (O/W) emulsion whereas one that consists of water droplets dispersed in an oil phase is called a water-in-oil (W/O) emulsion. Though thermodynamically unstable, an effective formulation can ensure kinetic stability against droplet coalescence and macroscopic phase separation (sedimentation or creaming) for the lifetime of the emulsion. This is accomplished by adding surfactants that lower the interfacial tension of the liquid-liquid interface. Biopolymers such as proteins and polysaccharides are also commonly used for their thickening ability [4].

Solids-stabilised or Pickering emulsions are defined as emulsions that are stabilised by the presence of colloidal particles situated at the oil-water interface [5]. The advantages of using particles as emulsifiers stem from their ability to help generate dispersed droplets with narrow size distributions, and the possibility of inverting emulsions from O/W to W/O systems by changing the particulate material [5].

Colloidal particles in the nanometre and micron range such as silica particles [6], polystyrene latex particles [7], and disk-like clay particles [8] have been used for emulsion stabilisation in the pharmaceutical and petrochemical fields. In foods, particles such as fat crystals and starch granules have been used as emulsifiers to improve the quality, appearance, and taste of many food products [9].

The capacity of fat crystals to stabilise dispersed aqueous droplets in food emulsions has been well-established [10-18]. They can effectively partition to the water-oil interface and create a stable emulsion. The stability of the resulting emulsions depends on their inherent properties, *e.g.*, morphology and concentration. Based on these findings, one may propose that similar functionality should be possible with solid lipid nanoparticles (SLNs).

This thesis aims to demonstrate that sub-micron colloidal particles, *i.e.*, SLNs, generated using microemulsion-based 'nanoreactors' can be used to stabilise W/O Pickering emulsions.

1.1 Fundamentals of colloidal systems

In this study, three colloidal systems were formulated and characterised, namely the microemulsions used as the 'nanoreactor', the resulting SLNs and finally, SLN-stabilised W/O emulsions.

1.1.1 Colloidal interactions – DLVO theory

The classical approach to describe the interaction between particles is the DLVO theory, named after Derjaguin, Landau, Verwey, and Overbeek [19-21]. This theory states that the stability of a colloidal system is determined by the sum of the van der Waals attractive and electrical double layer repulsive forces that exist between particles as they approach each other. The DLVO theory applies to non-Brownian particles, but other phenomena, such as gravity-

induced flocculation, may promote aggregation [22]. This theory states that a repulsive energy barrier prevents two approaching particles from adhering to one another (Fig. 1-1). If the particles collide with sufficient energy to overcome the barrier, the attractive force will pull them into contact, perhaps irreversibly. If the resulting particles have a sufficiently high repulsion, they will resist flocculation and the colloidal system will be stable. However, if repulsion does not exist, or is insufficient, then flocculation or coagulation will eventually take place.

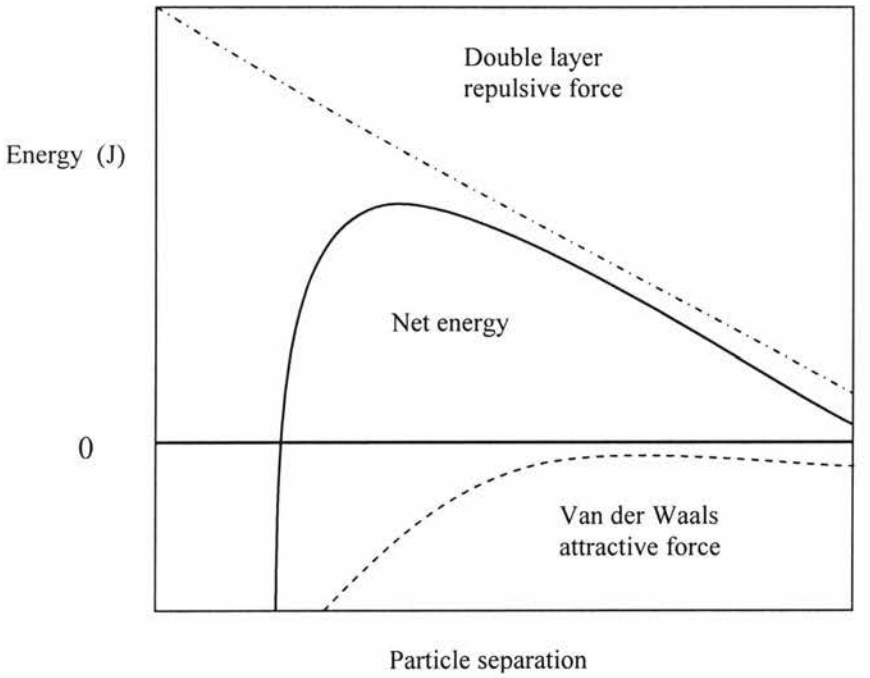

Figure 1-1: Schematic diagram of the variation in energy with particle separation, according to the DLVO theory. The net energy is given by the sum of the double layer repulsion and the van der Waals attractive forces that the particles experience as they approach one another (adapted from http://www.malvern.com/LabEng/industry/colloids/dlvo_theory.htm).

1.1.2 Instability of lipid-based colloids

The stability of colloidal lipid systems such as microemulsions, SLNs and macroemulsions changes over time due to the various physical processes, namely creaming, sedimentation, flocculation, coalescence, Ostwald ripening and phase inversion [23, 24]. In practice, these mechanisms may act in concert and influence one another.

1.1.2.1 Creaming and sedimentation

Creaming and sedimentation are a form of macroscopic phase separation where colloidal particles or droplets rise or sink due to density differences. If the droplets have lower density than the surrounding liquid, they tend to move up (creaming), and conversely, if they have higher density they tend to move down, resulting in sedimentation. Thus droplets in an O/W emulsion tend to cream, whereas those in a W/O emulsion tend to sediment.

1.1.2.2 Flocculation and Coalescence

Though these two processes initially occur at the micron scale, they eventually have repercussions on the macroscopic stability of an emulsion. Droplets in colloidal systems are in continual motion due to their thermal energy, gravitational forces, or applied mechanical forces, and as they move about, they collide with their neighbours. After a collision, droplets may either move apart or remain aggregated, depending on the relative magnitude of the attractive and repulsive forces between them. If the net force acting between the droplets is strongly attractive, they will aggregate, but if it is strongly repulsive, they will remain separated. Two types of aggregation are commonly observed in colloids: flocculation and coalescence.

In flocculation (Fig. 1-2), two or more droplets come together to form an aggregate in which the droplets retain their individual integrity, though they may be re-dispersed with agitation.

Extensive flocculation will lead to creaming as the droplets behave as a larger droplet. Coalescence is the process whereby two or more droplets merge to form a single layer droplet (Fig. 1-2). Any factor that increases the collision frequency is likely to increase the aggregation rate [23, 24].

1.1.2.3 Partial coalescence

Partial coalescence occurs when two or more partially crystalline droplets encounter each other and form a single irregularly-shaped aggregate [23]. Partial coalescence occurs only when the droplets have a certain solid fat-liquid oil ratio. If the solid fat content of the droplets is either too low or too high, the droplets tend not to undergo partial coalescence [24].

1.1.2.4 Ostwald ripening

Ostwald ripening is the growth of large droplets at the expense of smaller ones. This process occurs because the solubility of the material in a spherical droplet increases as the size of the droplet decreases [23,24]. The greater solubility of smaller droplets means that there is a higher concentration of solubilised material around a small droplet than around a large one. Thus, solubilised molecules travel from small droplets to large droplets given this concentration gradient, which causes the larger droplets to grow at the expense of the smaller ones.

Ostwald ripening also occurs with solid particles, as larger particles are more energetically favoured than their smaller counterparts. Molecules on the surface of a particle are typically less stable than those present within its interior [25].

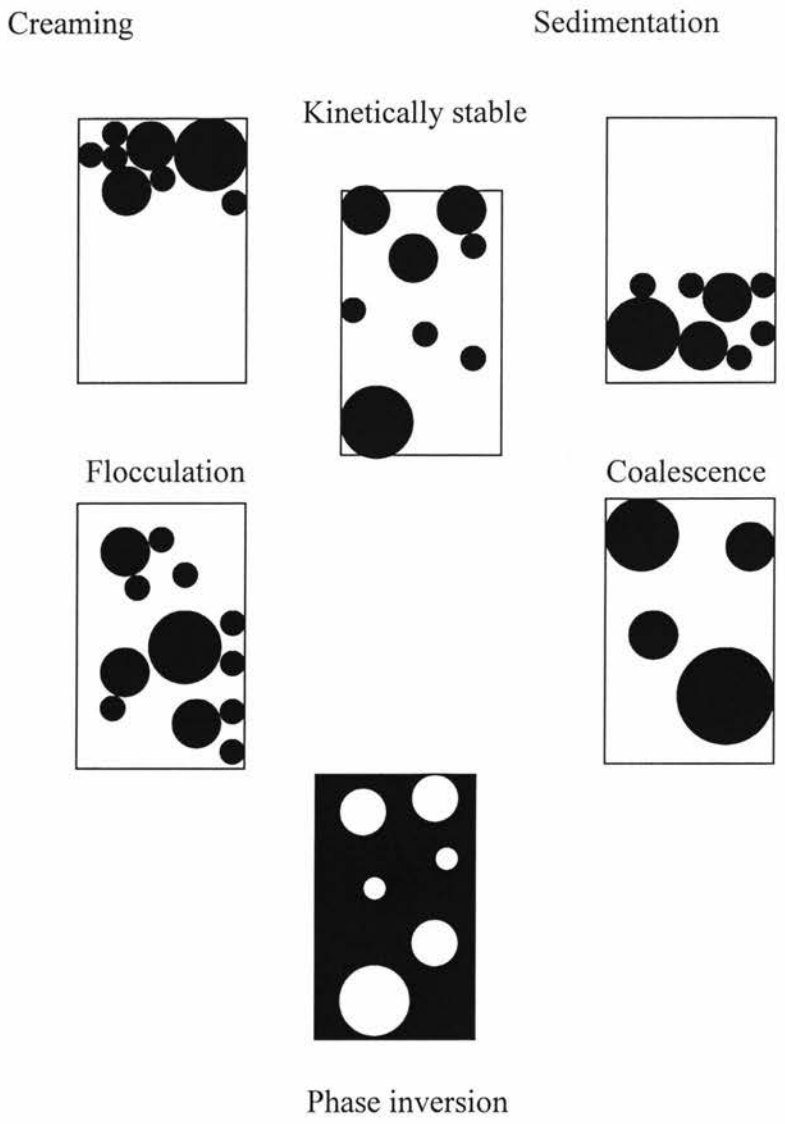

Figure 1-2: Mechanisms of emulsion instability (adapted from ref # 23)

1.1.2.5 Phase inversion

During phase inversion, a system changes from an O/W to a W/O emulsion or *vice versa*. This process usually occurs as a result of some alteration in the system's composition or environment, such as changes in dispersed phase volume fraction, emulsifier type/concentration or temperature.

1.1.3 Improving colloidal stabilisation

The above section has highlighted factors to be considered when predicting the stability of colloidal dispersions. This section discusses methods that can be used to stabilise emulsions. Other than adjusting the viscosity of the two phases or reducing particle size so as to prevent gravitational separation (creaming and sedimentation), improving the stability of colloidal systems usually focusses on the introduction of a repulsive force between the droplets or particles. The repulsion potential for droplets/particles covered with mono- or multi-molecular surfactant layers is obtained by adding a charged surfactant or a mixture of surfactants that can stabilise the system via electrostatic repulsion between dispersed droplets or particles.

From a thermodynamics viewpoint, a molecular assembly tends to organise itself so that the molecules are in an arrangement that minimises the Gibbs free energy (ΔG) of the system [26]. In emulsions, the Gibbs free energy is greater than zero and depends on interfacial energy ($\gamma \Delta A$) and the entropy of droplet formation ($T\Delta S$):

$$\Delta G_{emulsion\ formation} = \gamma \Delta A - T\Delta S_{emulsion\ formation} \qquad (1\text{-}1)$$

where γ is the interfacial tension, ΔA is the interfacial area, T is the temperature and ΔS is the configurational entropy of the system. When an emulsion is created by dispersing one immiscible liquid in another in the form of droplets, there is a great increase in interfacial area. The large positive interfacial energy term $\gamma \Delta A$ outweighs the entropy of droplet formation $T\Delta S$, which is also positive. This state is thermodynamically unstable. When a surfactant is introduced into an emulsion, the individual molecules adsorb on to the liquid-liquid interface and form a barrier that protects the droplets from aggregation, flocculation and/or coalescence [2,3]. The adsorption of surfactant molecules reduces the interfacial tension and the

thermodynamic instability caused by the increase in surface area. Thus, surfactant molecules shift the system towards a lower and more stable, though not thermodynamically stable, state. In microemulsions, the configuration entropy ($T\Delta S$) can dominate the interfacial free energy ($\gamma\Delta A$) in which the interfacial tension is extremely small due to the fairly high amount of surfactant (several percent). By lowering the interfacial tension, the droplet size is reduced and when it reaches the nanometre scale ($< \sim 200$ nm), a thermodynamically stable microemulsion forms spontaneously [26]. In addition, the small droplet ('domain') size and the dense adsorbed layer of surfactant (and co-surfactant) ensure lack of deformation of the interface, lack of thinning and disruption of the liquid film between droplets and hence coalescence does not occur.

The final means of stabilisation against coalescence is by using interfacially-active solid ('Pickering') particles that form a mechanical barrier limiting flocculation and coalescence. This should not be confused with network stabilisation, where solid particles are aggregated into a solid network and encase the dispersed phase, preventing flocculation and coalescence. In the former, the particles adsorb at the oil-water interface and form a film (monolayer or multilayer) around the dispersed droplets [16-20]. In the latter, stabilisation arises when a 3-D network of particles develops in the continuous phase surrounding the droplets. However, it has been reported that when a 3-D network forms, a dense particle layer on droplet surfaces may still exist. Thieme *et al.* reported that the presence of a 3D network combining clay particles and magnesium aluminium hydroxide stabilised O/W emulsions [27-29]. Abend *et al.* used a mixture of two particles (hydroxide and montmorillonite clay) with opposite charges to stabilise O/W emulsions by providing a stabilising layer around droplets and a particle network in the aqueous phase retarded creaming [30].

1.2 Thesis objectives

In light of the current state of the literature, where SLNs have not been used for the stabilisation or dispersed systems, the overall objective of this thesis is to develop SLNs within microemulsions to be used for W/O emulsion stabilisation. The specific objectives are as follows:

1. To formulate a microemulsion system using a pseudo-ternary phase diagram and establish the phase behaviour of the system, specifically the O/W domain.
2. Utilise selected O/W microemulsion compositions as 'nanoreactors' to develop SLNs.
3. To compare the crystallisation behaviour of the lipid used for SLN formation, monostearin, in bulk and within the O/W microemulsion.
4. To generate and optimise the properties of the microemulsion-based SLNs, their extraction and concentration.
5. To use the SLNs as interfacially-active (Pickering) particles for the stabilisation of W/O emulsions.

1.3 Hypotheses

1. Stable food-grade O/W microemulsions can be formulated with monostearin as the oil phase, a non-ionic surfactant (Tween 20), ethanol as a co-surfactant and high-purity water.
2. The formulated microemulsions are capable of being used as a nano-scale 'reactor' to generate SLNs *via* a super-cooling procedure.

3. The generated SLNs are able to stabilise W/O emulsions *via* Pickering and fat crystal network stabilisation.

1.4 Methodology and approach

It is proposed that SLNs developed within microemulsions will be able to stabilise W/O emulsions. The characterisation of selected dilution lines within the one-phase region of the formulated ternary phase diagram that encompass oil-continuous, bicontinuous and water-continuous regions will be used to decide upon the suitable microemulsion system used to develop the SLNs. An understanding of the crystallisation behaviour of the lipid used for SLN formation will be key in tailoring the supercooling approach used to develop nanoparticles within the selected microemulsions. Well-characterised nanoparticles will then be used to stabilise W/O emulsions, which in turn will be characterised.

1.5 Thesis organisation

The thesis is divided into seven chapters organised as follows:

Chapter 1 briefly introduced the fundamentals of colloidal interactions, the thermodynamic stability of colloidal systems and the factors that influence their stability. Microemulsions were introduced as thermodynamically-stable systems that form spontaneously. The stabilisation mechanisms in conventional emulsions, microemulsions and solid-stabilised emulsions were discussed as well as the key concepts for proper colloidal formulation.

Chapter 2 presents recent work on Pickering emulsions and the factors that govern emulsion stability. Fat crystals and their mechanisms for stabilising W/O emulsions are explained. Afterwards, the use of fats for SLN formulation and usage in emulsion stabilisation are discussed. Microemulsions, their constituents and phase behaviour are explained so as to

provide a better understanding of the application of these colloidal systems for SLN production.

Chapter 3 presents the materials used in this study, namely monostearin as the oil phase in the microemulsions, water, and Tween 20/ethanol as surfactant/co-surfactant mixture. Lecithin is also discussed as an additive yielding enhanced stability in the developed SLN suspensions. The experimental techniques used throughout the course of this study are also discussed.

Chapter 4 covers the formulation and characterisation of the developed microemulsions. A thorough explanation of the microemulsions' phase behaviour and the developed ternary phase diagrams is presented.

Chapter 5 reports on the development and optimisation of the developed SLNs, including the protocols used to tailor their supercooling, crystallisation, and particle separation.

Chapter 6 presents the results and discussion concerning the feasibility of using the developed SLNs to stabilise W/O emulsions.

Chapter 7 summarises the results presented in the thesis and discusses their potential application in the context of proposed future studies in the area of solids-stabilised emulsions.

Chapter 8 highlights possible areas for future studies and what could be done to fine-tune this research.

Chapter 2

Literature review

The literature review is broken down into two parts. The first part looks at existing work in the area of solids-stabilised emulsions, specifically fat crystal-stabilised emulsions and part 2 serves as an introduction to the microemulsion constituents used and their phase behaviour in general, as well as SLNs as potential surface-active agents in Pickering emulsions.

2.1 Solids-stabilised emulsions

Solids-stabilised emulsions have widespread applications in industrial settings such as food, cosmetics, pharmaceutical, petroleum and agrochemical [14] and have a history dating back to 1903, when Ramsden first reported emulsion droplets stabilised by particles. Pickering (1907) conducted the first systematic study on these emulsions and recognised the role of finely divided insoluble emulsifiers. The contribution of his work led to the name 'Pickering emulsions' for solids-stabilised emulsions. These two classic studies demonstrated that the fine (nanometres to microns [5]) solid particles would remain at an oil-water interface and promote droplet stability [28]. A wide variety of solid particles have been used as stabilisers of either O/W or W/O emulsions including iron oxide, hydroxides, metal sulphates, silica, clays and carbon. The formation, stability and structure of Pickering emulsions have been studied extensively by Binks *et al.*, who explored the capacity of silica particles, polystyrene latex particles, and clay particles as stabilisers [6-9,27,31-33]. These authors showed that both W/O and O/W emulsions could be stabilised with this approach, but that emulsion stability was highly-dependent on the properties of the particles used [31-33].

Rousseau reviewed the key factors that determine the effectiveness of fat crystals as emulsion stabilisers in food systems [10]:

i) The wettability of the crystals at the interface;

ii) Interfacial film rheology;

iii) Particle microstructure;

iv) The location of the fat crystals in the dispersed phase or continuous phase.

These are now addressed in greater detail.

2.1.1 Particle wettability

As Pickering species, the role that fat crystals play on emulsion stability strongly depends on how they are wetted by the continuous or dispersed phase. During or after emulsification, particles may be adsorbed at the interface, particularly if they are surface-active. Adsorbed particles will be preferentially wetted by the aqueous or oil phase depending on the composition of the phase [*i.e.*, the presence and type of the emulsifier(s)] as well as the composition and surface properties of the particles. This behaviour is best described by the contact angle formed at the boundary of the three phases [10,11], where the contact angle is measured through the aqueous phase (Fig. 2-1). Hydrophilic particles with contact angles < 90° will tend to stabilise O/W emulsions whereas hydrophobic particles with contact angles > 90° will normally stabilise W/O emulsions.

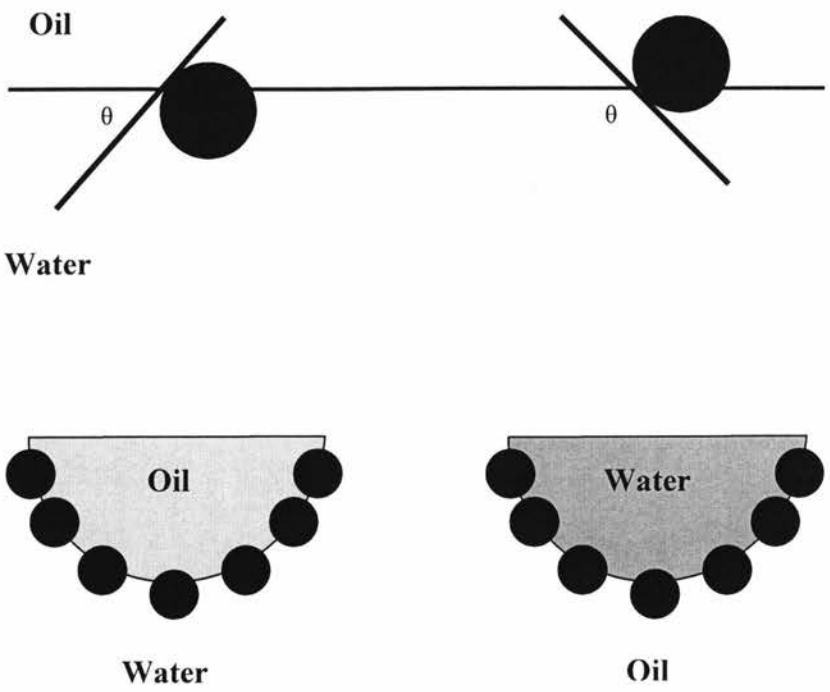

Figure 2-1: (A) Position of a small spherical particle at a planar oil-water interface for a contact angle (measured through the aqueous phase) < 90° (left), and > 90° (right). (B) Corresponding probable positioning of particles at a curved interface. For θ < 90°, solid-stabilised O/W emulsions may form (left). For θ > 90°, solids-stabilised W/O emulsions may form (right) (adapted from ref. #27)

If the particles are fully wetted by either the oil or aqueous phase, they will become fully dispersed in that phase and will not behave as Pickering species.

The contact angle depends on the surface free energies (interfacial tensions) at the particle-water, γ_{pw}, particle-oil, γ_{po}, and oil-water, γ_{ow}, interface according to Young's equation:

$$\cos\theta = \frac{\gamma_{po} - \gamma_{pw}}{\gamma_{ow}} \qquad (2\text{-}1)$$

When $\gamma_{po} = \gamma_{pw}$, the contact angle is 90°, which means the particle is wet equally by both liquids. Hydrophilic particles are wetted by water, therefore $\gamma_{po} > \gamma_{pw}$, and the contact angle will be $0° < \theta < 90°$. For hydrophobic particles, which will be wetted by oil $\gamma_{po} < \gamma_{pw}$, the contact angle will be $90° < \theta < 180°$.

The energy associated with the attachment and removal of theoretical spherical particles has been investigated by Levine *et al.* [12] and can provide a means of relating emulsion stability to observed interfacial tensions and contact angle measurements.

The energy of attachment of a particle to a fluid-fluid interface is related not only to the contact angle but also to the oil-water interfacial tension, γ. Assuming the particle is small enough so that the effect of gravity is negligible, the energy E required to remove a particle from an interface is given by:

$$E = \pi\alpha^2\gamma(1 \pm \cos\theta)^2 \qquad (2\text{-}2)$$

where α is the radius (m) of the particle and γ (mN m^{-1}) is the interfacial tension. The sign inside the bracket is negative for removal of particle from the interface into the water phase, and positive for removal of particle from the interface into the oil phase. Since E depends on the square of the particle radius, it decreases markedly with decreasing particle radius. Very small particles (< 5 nm) adsorb and desorb on a relatively fast timescale at an interface and may not be too effective as stabilisers [27].

The presence of charged surfactants will provide extra stability conferring a polar surface to fat crystals. Surfactants with greater polarity will adsorb more quickly compared to less polar surfactants. The different adsorption rates of lecithins with different polarities was studied by Johansson *et al.* [13, 34] who found that lecithins adsorb to fat crystals, making their surface more polar. This adsorption process is quick (< 5 min) for relatively polar lecithins, such as soybean phosphatidylcholine, and results in highly polar surfaces. Less polar lecithins adsorb slowly (hours) and result in less polar crystals.

2.1.2 Interfacial rheology

The interfacial layer at the droplet surface can exhibit viscous, elastic, and viscoelastic properties. In the presence of an interfacial particle film, an interface will begin to demonstrate viscoelastic behaviour. The ability of an emulsion to resist coalescence will depend largely on the properties of the interface. A highly viscous and rigid interfacial film laden with particles will retard film drainage and resist rupture, therefore promoting stability [10].

2.1.3 Particle size and morphology

Particle size is another factor that influences the interface, and therefore emulsion stability. Experimentally, it has been shown by Binks and Lumsdon [32] that decreasing particle size can lead to increased emulsion stability. In their study, average emulsion drop diameters initially increased from 35 to 75μm with increasing the particle diameter from 0.029 to 2.70 μm and then remained constant. Nanoparticles have also been used to stabilise Pickering emulsions, namely CdSe nanoparticles (1-8 nm) [35], silver nanoparticles (1-5 nm) [36] and clay particles (25-35 nm) [37].

Particle shape also influences emulsion stability. Well-defined spherical particles are often used for theoretical studies to simplify analysis and calculations. In practice, however, solid fat particles are not spherical. It has been shown that stable emulsions can be attained with non-spherical fine clay particles and fumed silica [28]. To date, no systematic study to elucidate the role of particle shape in emulsion stabilisation has been performed.

Studies have alluded to the role of particle roughness [38]. Particle roughness can also affect the apparent contact angle of particles and hence influence emulsion stability in the same manner as particle wettability. By comparing smoother spherical particles to smaller particles with noticeable roughness, Vignati *et al.* [38] determined that rougher particles produced less

stable emulsion droplets than when larger, smoother particles were used. The surface coverage of emulsion droplets with rough particles was very different from that with smooth particles. With the former, the surface coverage was much lower and particles were either grouped together or randomly distributed across the surface. By contrast, a high surface coverage and an even particle distribution were observed with smooth particles. Campbell [10] mentioned that fat crystal morphology could also affect emulsion stability, as the equilibrium position of crystals at the oil-water interface depended on particle microstructure.

2.1.4 Influence of particle concentration

The formation of a sufficiently dense layer of solid particles providing complete droplet coverage is necessary to stabilise an emulsion. Interfacial particle concentration will depend on the number of droplets and their size distribution. It has been shown that as the concentration of particles increases, the size of emulsion droplets decreases to accommodate more particles at the interface [28]. Tambe and Sharma [14] showed the existence of a limiting concentration such that any increase in the concentration of particles above this limit would not result in any smaller droplets or increased emulsion stability.

The importance of fat crystal concentration on the stability of water-in-triglyceride emulsions stabilised by monoglycerides was emphasised by Johansson *et al.* [15,16,27]. At low monoglyceride concentrations, flocculation and eventually coalescence of the water droplets were induced, whilst at higher concentrations, both were inhibited. These results were explained by a crossover in the mode of action of the crystals, in which they behaved as bridging particles between droplets when dilute (destabilisation) but formed a protective layer around droplets when concentrated (stabilisation).

Midmore [17] stabilised O/W emulsions with colloidal silica particles that covered only 29% of the oil droplets present. Additional silica increased the surface coverage, resulting in 80% coverage at the highest silica concentration, but did not result in a stable emulsion. This was explained as a result of the saturation of droplets with silica particles.

Vignati *et al.* [38] provided more evidence that emulsion stability can be achieved with coverage of only 5% of oil droplets using fluorescent silica particles, with higher concentrations not inducing complete droplet coverage.

2.2 Stabilisation of W/O emulsions by fat crystals

Fat crystals contribute to the stability of W/O emulsions by attaching themselves to the surface of aqueous droplets and protecting them against coalescence via Pickering stabilisation. The effectiveness of the crystals depends on their size, shape and morphology, as well as on the crystal surface wettability as influenced by the presence of other surface-active species. The effect of crystals surface polarity on the stability of W/O emulsions was demonstrated by Campbell [39]. Based on visual observation, emulsions made with 1 wt.% monoglyceride crystals were stable, whereas those made with 1 wt.% triglyceride crystals were not, which could be attributed to the high polarity of the monoglyceride crystals.

The influence of fat crystal concentration on W/O emulsion stability was systematically investigated by Johansson *et al.* [16,40]. They observed that water-in-soybean oil emulsions stabilised by monoolein without any fat crystals (palm stearin in the β′ polymorph) coalesced: ~60-70% of the dispersed aqueous phase had separated after 1 day. Stability was gradually improved by addition of palm stearin crystals to the oil. A particle content of >0.5 wt. % significantly lowered the sediment volume. With a particle content of 3-4 wt. %, no phase separation was visible within 1 week, and only 10-20% of the water separated after 1 month.

The effect of particle size on emulsion stability was studied by Garti *et al.*, [18], who observed that crystals ranging from < 1 μm up to 18 μm in size could kinetically stabilise emulsions. Larger crystals did not effectively adsorb to the interface and flocculated as free crystals in the continuous phase.

2.2.1 Stabilisation mechanisms

Fat crystals can enhance W/O emulsion stability via either Pickering stabilisation or the presence of a continuous phase fat crystal network. However, there is a concentration dependence to the stabilisation. At lower concentrations (< 1wt.%), based on the findings of Johansson *et al.*[16,41], fat crystals may have a detrimental effect on emulsion stability due to insufficient droplet coverage, which can lead to bridging flocculation (Figure 2-2(a)). This phenomenon results in enhanced coalescence, especially in the presence of a shear field whereby breaking the fat crystal film layer around the droplets increases droplet-droplet collisions. At higher crystal concentrations, *e.g.*, ≥ 2 wt.%, (Figure 2-2(b)), crystals inhibit coalescence by preventing droplets from touching each other.

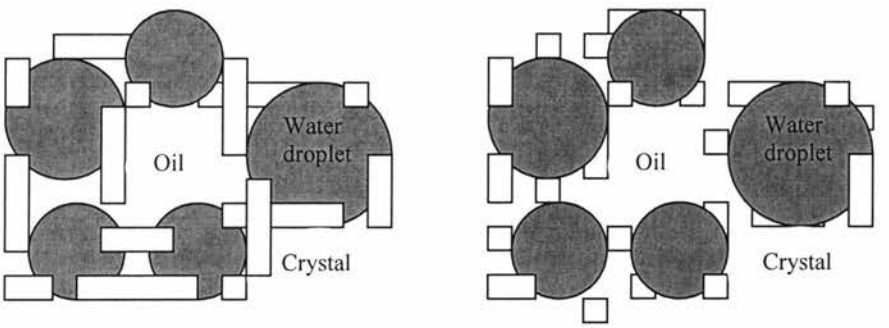

Figure 2-2: Highly schematic representation of the effect of the distribution of fat crystals on the stability of water droplets dispersed in oil. (a) Bridging flocculation at fat crystal contents well below full saturation coverage of the oil-water interface, and (b) inhibition of coalescence due to screening of droplets with fat crystal contents near full saturation coverage. Adapted from ref. # 50

When an emulsion is prepared with a concentration of crystals below that corresponding to saturation coverage of the oil-water interface, destabilisation occurs due to combined sedimentation, flocculation and coalescence. Once saturation coverage has been reached as a result of loss of interfacial area, further coalescence is inhibited by Pickering stabilisation and potentially network stabilisation [16, 39, 40, 42].

2.3 SLN production methods

SLNs are made from solid lipids (lipids which are solid at room temperature and also at body temperature). The lipids can be highly purified triglycerides, complex glyceride mixtures, surface-active species or even waxes [43]. The physico-chemical stability of these lipid particles has been investigated extensively by Heurtault *et al.* [44]. Different approaches exist for the production of finely dispersed lipid nanoparticles, including: high pressure homogenisation, solvent emulsification-evaporation or diffusion, high speed stirring and/or ultrasonication, preparation by water-oil-water double emulsions, and via microemulsions. The group of Gasco developed and optimised a method for the preparation of SLN via microemulsions which has been adapted or modified by different labs [43,45-50]. To form a microemulsion with a solid lipid, the microemulsion needs to be produced at a temperature above the melting point of the lipid. The lipid is melted, and blended with a mixture of water, surfactant and co-surfactant heated to the same temperature. A transparent, thermodynamically stable system is formed when the compounds are mixed in the correct ratio for microemulsion formation. This microemulsion is then dispersed in a cold aqueous medium (2-4 °C) under mild mechanical mixing, thus ensuring that the small size of the particles is due to the precipitation and not mechanically induced by the stirring [47,51]. Nano-scale liquid oil domains present in the warm microemulsion

are quenched in cold water, which permits the crystallisation of oil droplets thus forming the solid nanoparticles [52].

2.4 Microemulsion constituents and phase behaviour

Microemulsions are dispersions of either 'water in oil' or 'oil in water' domains stabilised by a surfactant and co-surfactant mixture that significantly lowers the oil-water interfacial tension [53,54-63]. The resultant microemulsions are isotropic, normally of low viscosity and thermodynamically stable (Chp. 1, section 1.1.3). Their average particle size is usually 5-100 nm. W/O microemulsions are similar to reverse micelles, where the polar head group of the surfactant is oriented inward and the non-polar tail is oriented towards the oil continuum. O/W microemulsions are similar to normal micelles, where the non-polar tail of surfactant is oriented inward and the polar head group is oriented toward the aqueous continuous phase (Fig. 2-3). The difference between micelles and O/W microemulsions is that micelles form according to the aggregation behaviour of surfactant in water whereas in O/W microemulsions, the same structure is formed in the presence of both water and oil phases, with the surfactant molecules located at interface of the two phases.

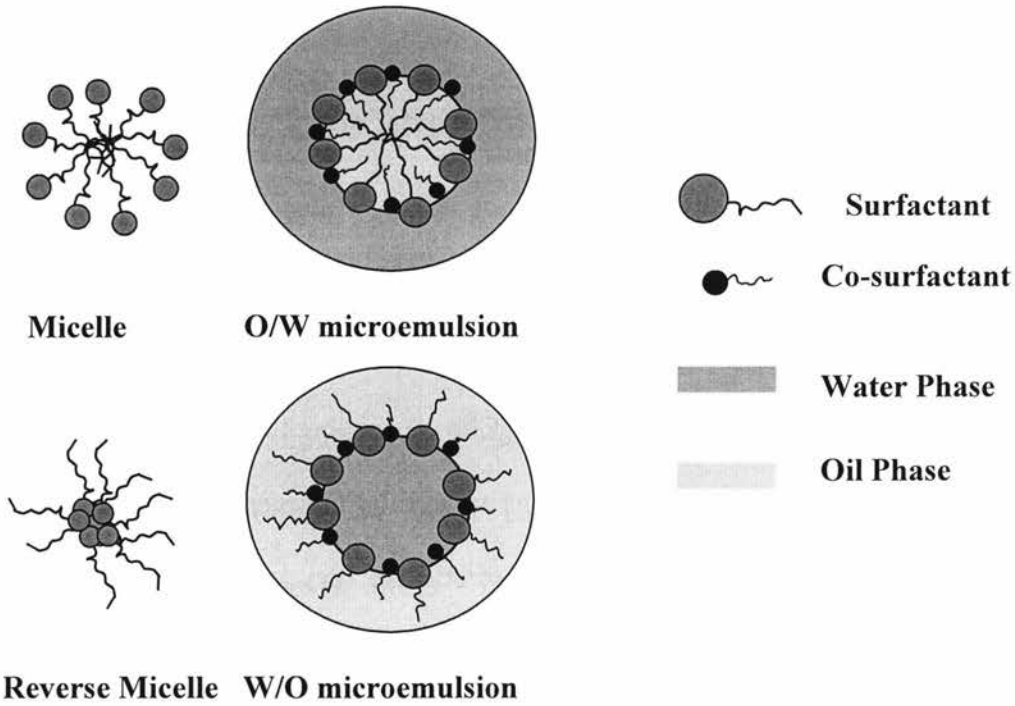

Figure 2-3: Pictorial representations of micelles, reverse micelles and microemulsions (adapted from ref. #53)

2.4.1 Phase behaviour

Ternary mixtures of water, surfactant and oil or quaternary mixtures of water, surfactant, co-surfactant and oil will generate unique phases, as described by Winsor [64] (Fig. 2-4):

1. two phases: a (O/W) microemulsion phase is in equilibrium with the upper excess oil (Winsor I).

2. two phases: the microemulsion phase (W/O) is in equilibrium with excess water (Winsor II).

3. three phases: the middle microemulsion phase (O/W, bicontinuous or W/O microemulsion) in equilibrium with upper excess oil and lower excess water (Winsor III).

4. single phase: oil, water and surfactant mixed (Winsor IV).

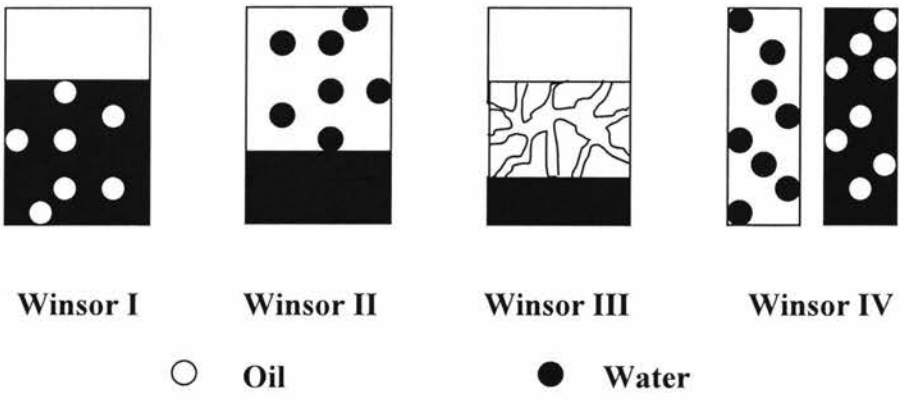

Figure 2-4: Possible water-surfactant-oil mixtures (adapted from ref. # 53, 64)

2.4.2 Phase structure

Microemulsion structures are often characterised as water-continuous (O/W), oil-continuous (W/O), or bicontinuous. These structures are influenced by the proportion of each microemulsion component (water, oil, surfactant, and cosurfactant).

Ternary phase diagrams have been used extensively in the study of microemulsions to explain their phase structure and phase transitions from W/O to bicontinuous to O/W microemulsions. In Fig. 2-3, an outline of the composition-dependent structures of a microemulsion system in a putative ternary phase diagram is shown:

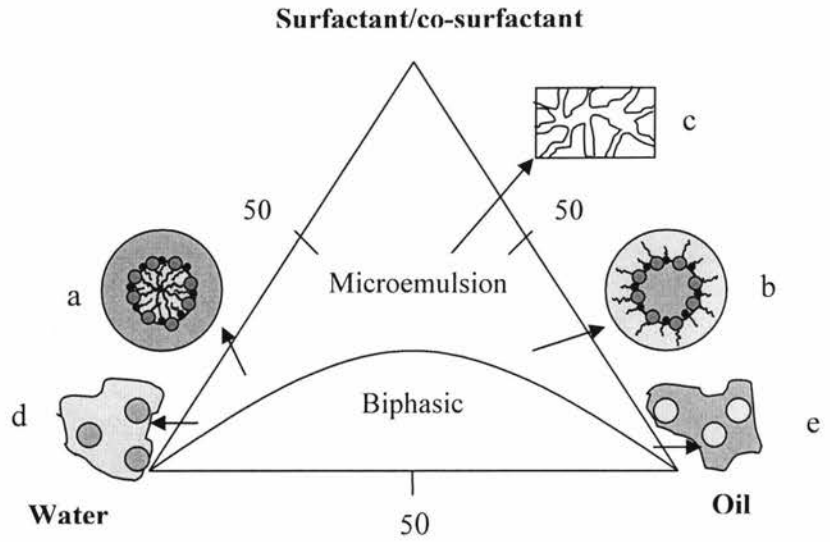

Figure 2-5: Comprehensive ternary phase diagram showing probable internal structures: (a) O/W microemulsion; (b) W/O microemulsion; (c) bicontinuous dispersion; (d) isolated and aggregated O/W dispersion; and (e) isolated and aggregated W/O dispersion. (adapted from ref. #53).

A number of studies on microemulsion phase behaviour (Chp. 4) have focussed on using non-ionic surfactant/alcohol mixtures for stable microemulsion formation [57-59,65,66], including different types of polyoxyethylene surfactants (Tweens) in combination with alcohols such as ethanol, butanol, and/or propylene glycol.

2.4.3 Monostearin

Monostearin ($C_{21}H_{42}O_4$, MW: 358.56, m.p: α-form polymorph melting point: 74 °C, β-form polymorph melting point: 81 °C) or glycerol monostearate (Fig. 2-6) is one of the most common naturally occurring monoacylglycerols. Commercially, monostearin is made by esterification of stearic acid ($C_{18}H_{36}O_2$) with glycerol at elevated temperatures or from glycerolysis with stearic acid, *i.e.*, the transestrification of stearic acid with glycerol [67]. Two types of monoacylglycerols exist depending on where the acyl group is attached on the

glycerol, 1-monoacylglycerol (α-monoacylglycerol) and 2-monoacylglycerol (β-monoacylglycerol) [68].

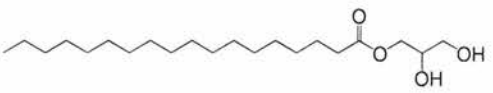

Figure 2-6: Chemical structure of 1-monostearin (adapted from sigmaaldrich.com).

Given the presence of the acyl chain and hydroxyl groups, monostearin shows strong surface activity. Since it is mostly lipophilic, it is soluble in oil and insoluble in water. It strongly adsorbs at the oil-water interface and acts as an emulsifier in W/O emulsions. Similar to other emulsifiers, monostearin is found in the oil-water interface with its polar headgroup (hydroxyl groups) oriented towards the aqueous phase and the non-polar group (the fatty acid-hydrocarbon chain) towards the lipid phase. In this manner, monostearin reduces the interfacial tension and stabilises emulsions. Its lipophilic character (Hydrophile/Lipophile Balance (HLB) value = 3.6-4.2) results in monostearin being an excellent W/O emulsifier.

There are many applications of monostearin in cosmetics, the medical field, pharmaceuticals and in the food industry. For example, monostearin SLNs have been used for the controlled delivery of drugs [69,70].

2.4.4 Polyoxyethylene (20) sorbitan monooleate (Tween 20)

Surfactants are surface-active molecules that consist of a hydrophilic head group attached to a lipophilic tail group. The head group may be anionic, cationic, zwitterionic, or non-ionic [71]. In Tween 20 ($C_{58}H_{114}O_{26}$) (Fig. 2-7), the headgroup possesses a sorbitan ring attached to 20 oxyethylene groups with no electrical charge so it is categorised as a non-ionic surfactant. The tailgroup consists of a hydrocarbon chain.

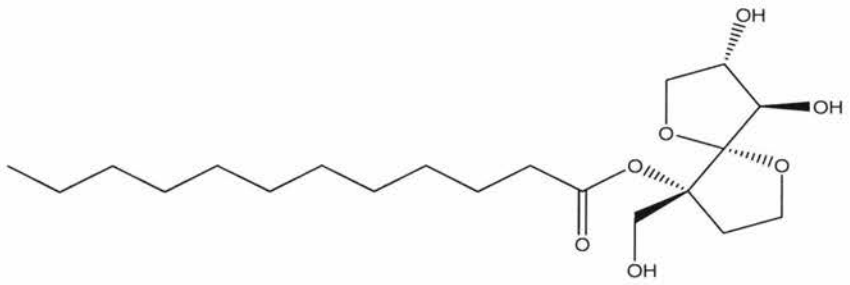

Figure 2-7: Oxyethylene sorbitan monolaurate (Tween 20) possesses 20 oxyethylene groups attached to a sorbitan ring) (adapted from sigmaaldrich.com).

One of the important functional properties of surfactants is their aggregation behaviour [72]. At sufficiently low concentrations, surfactants exist as monomers in solution as the entropy of mixing outweighs the attractive forces between the surfactant molecules [41]. As their concentration is increased to a critical level known as critical micelle concentration (CMC), they aggregate into micelles or reversed micelles (Fig. 2-1). A surfactant with a low HLB value (3-6) is predominantly hydrophobic, preferentially dissolves in oil, stabilises W/O emulsions, and forms reverse micelles in oil. A surfactant with high HLB number (10-18) is predominantly hydrophilic, preferentially dissolves in water, stabilises O/W emulsions, and forms micelles in water. With HLB values of ~16, Tween 20 is as a hydrophilic surfactant that preferentially stabilises O/W emulsions and forms micelles. The micelle formation property of surfactants makes it possible for non-polar molecules, which are normally insoluble or only sparingly soluble in water, to be 'solubilised' within an aqueous surfactant solution by being incorporated into the core of micelles [73]. Micelles containing solubilised materials are referred to as swollen micelles or microemulsions.

Tween 20 has GRAS (generally regarded as safe) status and has been used in numerous microemulsion formulations [63,74,75].

2.4.5 Ethanol

The effect of alcohols on the properties of micellar solutions has been the subject of extensive investigation [76]. Short-chain alcohols normally increase the CMC of surfactant solutions as they interact with water. As a result, their presence modifies the behaviour of water as the solvent, often making it more compatible with surfactant molecules. The presence of either short or long chain alcohols thus promotes microemulsion formation [60,62].

Ethanol (C_2H_5OH), a food-grade alcohol, has been used as a co-surfactant in many microemulsion formulations [66,74,77]. El Maghraby [78] observed that the incorporation of ethanol increased the size of the microemulsion region within ternary phase diagrams.

2.4.6 Lecithin

Lecithins are naturally-occurring surface-active molecules that can be extracted from different sources, including soybeans or eggs. Soy lecithin is the most widely used surfactant ingredient, especially in the food industry. Natural lecithins are a complex mixture of different phospholipids and other lipids, with the most common phospholipids being phosphatidylcholine (PC), phosphatidyletanolamine (PE) and phosphatidylinositol (PI). The hydrophilic head groups of these molecules are either anionic (PI) or zwitterionic (PC and PE), while the lipophilic tail groups consist of two fatty acids [71] (Fig. 2-8).

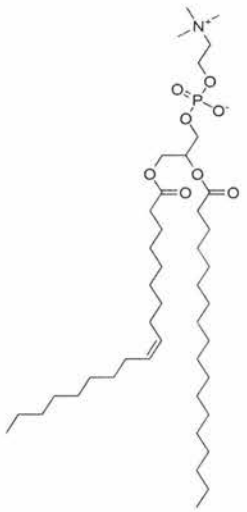

Figure 2-8: Lecithin structure showing the choline and phosphate polar headgroup and two apolar hydrocarbon chains (adapted from elmhurst.edu/images/553lecithin.gif)

As described later, lecithin was found to stabilise the monostearin nanoparticles herein developed as its charge properties reduced SLN coalescence via electrostatic repulsion (Chp. 1. Section 1.1.3). Lecithin has previously been used to stabilise SLN dispersions [79,80]. You *et al.* were able to improve SLN particle size and stability via cold homogenisation in the presence of lecithin [79]. In another study, conducted by Battaglia [80], soy lecithin and taurodeoxycholate (TDC) were used to stabilise glycerol monostearate nanoparticles.

Chapter 3

Experimental methods

The following chapter introduces each of the experimental methods used to formulate and characterise the microemulsions, SLNs and the W/O Pickering emulsions. Specific measurements associated with each experiment are addressed within the experimental sections of the subsequent chapters. Unless otherwise indicated, all experiments within this thesis were performed in triplicate, as were their respective measurements.

3.1 Microemulsion preparation

The physical and chemical properties of the microemulsion components including monostearin, Tween 20 and ethanol have been thoroughly described in the literature [41,67,68,71-73,76]. The monostearin used in all experiments was Pationic 901 (>95% purity, Caravan Ingredients K.S., USA). Tween 20 (Sigma-Aldrich, St. Louis, USA) had an HLB value of 16.6 and CMC value of 60 mg/l. The ethanol with 100% purity was from Commercial Alcohols Inc. (Brampton, ON, Canada). Reverse osmosis water from the Food Research Laboratory at Ryerson University was used for all experiments.

Monostearin was melted and mixed with a heated mixture of surfactant and co-surfactant at different ratios. In order to construct pseudo-ternary diagram to study the phase behaviour, water was added at 10% to 90% (w/w) to the above mixture at the same temperature. A transparent sample indicated microemulsion formation. All samples were prepared in test tubes and sealed with screw-caps, and allowed to equilibrate 24 h.

Pseudo-ternary phase diagrams with the four components (monostearin, Tween 20, ethanol, and water) were constructed to study their phase behaviour. Phase transitions were

examined visually by the appearance of cloudiness or sharply defined separated phases. The phase diagrams were constructed at 70 °C. As discussed later in Chapter 4, the top apex represented the Tween (20)/ethanol mixture and the other two apices were monostearin and water.

3.2 SLN development

The SLNs were prepared by super-cooling the O/W microemulsions. In order to stabilise the monostearin crystals, 0.5% granular lecithin (Acros Organics, >97% purity) was added to the prepared warm microemulsion. The addition of lecithin did not greatly affect the phase behaviour of the O/W microemulsions (Chp. 5). The warm microemulsion doped with lecithin was poured into cold water (2-4°C) at a 1:10 ratio, while stirring with a magnetic stirrer at ~300 rpm, until the appearance of a milky solution (30-45 min), indicative of monostearin solidification.

The prepared SLNs were centrifuged for 2 × 30 min at 3500 rpm (IEC-Centra-CL2 centrifuge, International Equipment Company, MA. USA) until a visually clear solution separated from the precipitated solid material (45 ml). The supernatant was separated and the solid precipitate was collected. This approach resulted in ~90 mg of SLNs in each tube.

3.3 W/O emulsion preparation

Emulsions were prepared using an impeller-type homogeniser (Omni-Mixer Homogeniser; London Scientific, London, Ontario, Canada), which had a micro-attachment containing a blade-type impeller (total cell volume = 5 ml), operated at ~5000 rpm for 1 minute to pre-blend followed by 5 minutes at ~27,000 rpm to homogenise. All emulsions consisted of 20% water, SLNs at different concentrations [0.5, 1, 1.5 and 2 % (w/w)] with the oil phase consisting of light mineral oil (>99% purity, Fisher Scientific, NJ, USA). The sample

cell was kept in an ice bath during homogenisation to prevent large temperature increases – an average temperature of ~19 °C was maintained during mixing. This homogeniser was chosen to prepare the emulsions as it allowed for small sample volumes (5 ml).

3.4 Dynamic light scattering

Dynamic light scattering (DLS) (sometimes referred as photon correlation spectroscopy or quasi-elastic light scattering) is a technique often used for measuring sub-micron particle sizes. Here, it was used to measure particle size, zeta potential and conductance. For particle sizing, DLS measures the Brownian motion of particles and relates this to their size. Particle size is determined based on the Stokes-Einstein equation, where Brownian motion is dependent on the diffusion coefficient:

$$d = \frac{kT}{3\pi\eta D} \tag{3-2}$$

Here, d is the hydrodynamic diameter (nm), k is Boltzmann's constant (1.38054×10^{-23} J/K), T is absolute temperature (K), η (centipoise) is viscosity and D (cm^2/sec) is the diffusion coefficient. The instrument used was a Brookhaven 90Plus/BI-MAS DLS (Brookhaven Instruments Corporation, Holtsville, NY, USA). The DLS also provided the polydispersity index, which is the breadth of the particle size distribution. This measurement was used to characterise the particles both within the microemulsions and final SLN systems.

The zeta potential (in mV) provides a measurement of the surface charge of a particle. In an applied electric field, charged particles will move towards either the positive or the negative electrode of the applied field, depending on its surface charge. Conductance measurements, which were also obtained with the same instrument using the zeta potential mode, are a measure of how easily electrical current flows through a sample.

3.5 Viscosity measurements

The steady-state viscosity of the microemulsions along specific dilution lines was investigated with a controlled stress rheometer (C-VOR model, Malvern Instruments Ltd., Mississauga, Ontario, Canada), operating with a Cup and Mooney geometry. All measurements were performed at 70 °C.

3.6 Differential scanning calorimetry

Differential scanning calorimetry (DSC) is a thermal analysis technique used to measure the energy necessary to establish a close to zero temperature difference between a sample and empty reference pan. The sample and reference are both maintained at a temperature predetermined by the programme, even during a thermal event in the sample. The amount of energy which has to be supplied to or withdrawn from the sample to maintain a zero temperature gradient between the sample and reference is the experimental parameter displayed as the ordinate of the thermal analysis curve. Whether more or less heat must flow to the sample depends on whether the transition is exothermic or endothermic. For example, a solid-to-liquid transition, which requires heat, is an endothermic process whereas crystallisation, which is a liquid-to-solid transition, is exothermic. Any transition accompanied by a change in specific heat is demonstrated as peaks whose areas are proportional to the total enthalpy change [56].

DSC measurements were performed with a Perkin-Elmer Pyris-Diamond DSC (Markham, ON, Canada). The samples were weighed using a Mettler M3 microbalance in DSC aluminum pans, and then sealed using a universal press (B013-9005, Perkin Elmer, Markham, ON, Canada). An empty sealed pan was used as reference.

3.7 Confocal laser scanning microscopy

Polarised light microscopy (PLM) and confocal laser scanning microscopy (CLSM) [81] were used to examine the dispersed phase of the W/O emulsions, along with the possible presence of SLNs at the oil-water interface.

A Zeiss Axioplan-2 microscope equipped with a LSM 510 confocal module and the associated software (version 3.2; Zeiss Instruments, Toronto, ON, Canada) were used together with a 63× Achroplan water-immersion objective. Emulsion samples were prepared as previously mentioned (section 3.3), except that the fluorescent stains Rhodamine B (Acros, NJ, USA) and Fluorol Yellow 088 (Sigma-Aldrich, St. Louis, USA) were added to the water and oil phases respectively, at 0.01% (w/w). Rhodamine B was excited at 543 nm and Fluorol Yellow 088 at 488 nm, with the emitted light passing through an LP 560 filter for detection. Welled glass slides (depth = 0.5mm) were used to load samples for microscopy.

3.8 Contact angle measurements

The contact angle as described in Chapter 2 is a critical parameter in the design of a Pickering emulsion and establishes the position of interfacial particles relative to the oil-water interface. In order to measure contact angle, monostearin was melted at ~ 75°C while stirring and poured into aluminium weigh boats at room temperature and allowed to crystallise for ~ 3 h. The solidified disks were then cut into ~1 cm cubes and placed in spectrophotometer cuvettes, with the smooth side facing upwards. Cuvettes were then filled with light mineral oil. A small droplet (~ 1 mm o.d) of water was then injected from a needle (gauge 22, Fisher Scientific, 0.711 mm nominal outer diameter and 0.394 mm nominal inner diameter) onto the surface of the solid fat using a 10 ml syringe and a programmable syringe pump (kd Scientific, Markham, ON, Canada) operated at 0.1 ml/min. Images of the water droplet were captured

with a Teli CCD camera with macro lens assembly and IDS Falcon/Eagle framegrabber (DataPhysics Instrument GmbH, Filderstadt, Germany) for up to 5 d. Image analysis to determine the contact angle of the droplet against the solid surface was performed using SCA 20 version 2.1.5 build 16.

3.9 Emulsion droplet size distribution

A Bruker Minispec Mq pulsed nuclear magnetic resonance (pNMR) unit (Bruker Canada, ON, Canada) equipped with a pulsed field gradient (pfg) unit was used to characterise the size distribution (DSD) of the SLN-stabilised W/O emulsion droplets. The principle is based on the restricted diffusion of water molecules [82-84]. Briefly, pfg-NMR self-diffusion measurements of hydrogen nuclei take place when two equal field gradient pulses are applied within a standard spin-echo pulse sequence, where the intensity of the observed echo is reduced by the effect of molecular diffusion. Within emulsion droplets, diffusion is restricted by the presence of the interface. Once this boundary is reached, the echo intensity is no longer reduced. Thus, by monitoring signal attenuation as a function of gradient strength, one may determine droplet sizes within an emulsion and thus generate a droplet size distribution. As this technique relies on the molecular movement of water molecules within droplets, it detects size increases in the droplets themselves and not the clustering of droplets, thereby differentiating between coalescence and flocculation or coagulation.

The pfg-NMR field gradient strength was calibrated with $CuSO_4$–doped water [diffusion coefficient (D) = 1.31 x 10^{-9} m^2/s at 5 °C]. Emulsion samples were pipetted into NMR tubes (1 cm o.d, L=15 cm) for NMR droplet size analysis. The droplet sizes (volume-weight mean diameter (d_{33})) of the W/O emulsions were analysed within 1 hour of being made and at days 0, 1, 2, 4, 7 and 10.

3.10 Atomic force microscopy

The atomic force microscope (AFM) belongs to a family of versatile instruments called scanning probe microscopes designed to measure the surface properties of materials. It generates images by "feeling" the surface of a sample, using a sharp tip, akin to a stylus on a record player.

The anatomy of an AFM consists of three fundamental elements. The tip consists of an extremely sharp spike mounted onto the end of a cantilever. Tips are usually made from silicon or silicon nitride using semiconductor fabrication methods. The sharpness of the spike will strongly dictate the resolving ability of an AFM. The tip apex may be as small as 1 nm. It is the cantilever that allows the tip to move up or down and feel the contours of a sample's topography. Another important feature is the scanning mechanism, which controls the motion of the tip. The cantilever is controlled by a piezo-electric transducer capable of moving the tip at the atomic level in the X, Y and Z axes. The third key element of an AFM is the detection mechanism. As an AFM tip scans the surface of a sample, its motion must be detected. The most common detection method is the optical lever system whereby a laser diode is focused onto the mirrored end of the cantilever. Deflections resulting from changes in tip-sample interactions change the reflection angle of the laser beam, and hence laser intensity, which is monitored by a position-sensitive detector capable of detecting angstrom-scale bending motions. The signal from the detector is converted to an image visible on a computer monitor, where it can be digitally analysed [85].

Prepared SLN samples were mounted on mica slides and placed to air dry in a fume hood. Samples were examined under ambient conditions using a Bioscope atomic force microscope (AFM) with Nanoscope IIIa controller (Digital Instruments, Santa Barbara, CA,

USA), operated in tapping mode. The AFM tips had a cantilever spring constant of 40 N/m and were oscillated at ~350 kHz with an end-point radius of 10 nm and a body angle of 30°.

3.11 Data analysis

Results are reported in all experiments as arithmetic means ± standard deviation. Statistical analysis was performed using a two-tailed Student's *t*-test. Differences were considered statistically significant at $p \leq 0.05$.

Chapter 4

Formation and characterisation of food-grade microemulsions

4.1 Introduction

Microemulsions are nm-scale dispersions of either water-in-oil (W/O) or oil-in-water (O/W) droplets or bicontinuous structures stabilised by surfactants and co-surfactants. They form spontaneously and exhibit optical transparency and isotropy, low viscosity and thermodynamic stability. Their transparency is due to droplets ranging in size from 5 to 100 nm, which is smaller than the wavelength of visible light, ca. 400-700 nm [54]. Microemulsions have seen increased usage in cosmetics and pharmaceuticals, as well as in the food industry due to their physicochemical properties such as thermodynamic stability, high solubilisation capacity, transparency and low viscosity. For food applications, toxicity concerns limit the number of compounds that can be used in microemulsion formulations (*e.g.*, long chain alcohols or surfactants), though there has recently been progress made in this area [55-59].

Polyoxyethylene sorbitan esters (Tweens) are inexpensive and readily-available food-grade surfactants that can be used for microemulsion formation. They consist of bulky polyoxyethylene head groups attached to a sorbitan ring, which increases their hydrophilicity. There are numerous pharmaceutical application of O/W microemulsions using Tweens [65,93-97]. The addition of short-chain alcohols such as ethanol help in the formation of both W/O and O/W microemulsion [60,62,78].

The aims of this study were to: i) establish and characterise a food-grade microemulsion system using monostearin as the oil component, Tween 20 as a surfactant and

ethanol as a co-surfactant, ii) identify the types of microemulsions formed and iii) explore their potential as nanoparticulate reactors.

4.2 Experimental

4.2.1 Materials

The physical and chemical properties of the microemulsion components (monostearin, Tween 20, ethanol and water) and the microemulsion preparation method were described earlier in Chp. 2, Section 2.3 and Chp. 3 section 3.1 respectively.

4.2.2 Methods

4.2.2.1 Pseudo-ternary phase diagrams at constant temperature

The phase behaviour of a system consisting of water, oil, surfactant and co-surfactant may be described on a phase tetrahedron whose apices respectively represent the pure components. In a pseudo-ternary phase diagram, however, a fixed (weight, volume or mole) ratio of any of two components represents one of the apices. In this study, the mixture of surfactant and co-surfactant (Tween 20:ethanol) at a fixed ratio of 1.5:1 was used.

Mixtures consisting of monostearin and the Tween 20/ethanol mix at fixed ratios (1:9, 2:8, 3:7, 4:6, 5:5, 6:4, 7:3, 8:2 and 9:1 monostearin:Tween 20/ethanol) were prepared in test tubes and sealed with screw caps (Tab. 4.1). They were placed in a 80 °C waterbath until the monostearin had melted (30 min), at which point samples at each ratio were diluted with different amounts of hot (80 °C) water: 10-90% (w/w). Samples with the 7:3, 8:2 and 9:1 ratios of monostearin:Tween 20/ethanol were unstable, thus these compositions are not reported (Tab. 4.1).

Table 4-1: The composition of prepared microemulsion samples along dilution lines 10-90, 20-80, 30-70, 40-60, 50-50, and 60-40

Dilution line 10-90		
Monostearin (g)	**Tween 20:ethanol 1.5:1 (g)**	**Water (g)**
0.27	2.43	0.3
0.24	2.16	0.6
0.21	1.89	0.9
0.18	1.62	1.2
0.15	1.35	1.5
0.12	1.08	1.8
0.09	0.81	2.1
0.06	0.54	2.4
0.03	0.27	2.7

Dilution line 20-80		
Monostearin (g)	**Tween 20:ethanol 1.5:1 (g)**	**Water (g)**
0.54	2.16	0.3
0.48	1.92	0.6
0.42	1.68	0.9
0.36	1.44	1.2
0.31	1.19	1.5
0.24	0.96	1.8
0.18	0.72	2.1
0.12	0.48	2.4
0.06	0.24	2.7

Dilution line 30-70		
Monostearin (g)	**Tween 20:ethanol 1.5:1 (g)**	**Water (g)**
0.81	1.89	0.3
0.72	1.68	0.6
0.63	1.47	0.9
0.54	1.26	1.2
0.45	1.05	1.5
0.36	0.84	1.8
0.27	0.63	2.1
0.18	0.42	2.4
0.09	0.21	2.7

Dilution line 40-60		
Monostearin (g)	**Tween 20:ethanol 1.5:1 (g)**	**Water (g)**
1.08	1.62	0.3
0.96	1.44	0.6
0.84	1.26	0.9
0.72	1.08	1.2
0.59	0.91	1.5
0.48	0.72	1.8
0.36	0.54	2.1
0.24	0.36	2.4
0.12	0.18	2.7

Dilution line 50-50		
Monostearin (g)	**Tween 20:ethanol 1.5:1 (g)**	**Water (g)**
1.35	1.35	0.3
1.21	1.19	0.6
1.05	1.05	0.9
0.87	0.93	1.2
0.75	0.75	1.5
0.61	0.59	1.8
0.45	0.45	2.1
0.32	0.28	2.4
0.15	0.15	2.7

Dilution line 60-40		
Monostearin (g)	**Tween 20:ethanol 1.5:1 (g)**	**Water (g)**
1.62	1.08	0.3
1.44	0.96	0.6
1.26	0.84	0.9
1.08	0.72	1.2
0.91	0.59	1.5
0.72	0.48	1.8
0.54	0.36	2.1
0.36	0.24	2.4
0.18	0.12	2.7

All samples after addition of water were shaken vigorously to assure complete mixing. Samples were kept in a waterbath (70 °C) for 24 h, which was deemed sufficient to establish phase behaviour. Phase transitions were detected visually by the appearance of cloudiness or sharply defined separated phases. The phase diagrams were determined at 70 °C.

Pseudo-ternary phase diagrams were established with and without ethanol as co-surfactant at different Tween 20:ethanol ratios (1:2, 1:1.5, 1:1, 1.5:1 and 2:1) to determine the role of the co-surfactant in microemulsion formation and to determine the optimum surfactant:co-surfactant ratio.

4.2.2.2 Dynamic light scattering

A Brookhaven 90Plus/BI-MAS (Brookhaven Instruments Corporation, Holtsville, New York, USA) was used to measure the particle size (nm) and polydispersity of the microemulsions at 70 °C. Conductance (μS) was determined by using the ζ-potential mode. All measurements were performed after 24 h. The measured particle radius was used to calculate the diffusion coefficient using the Stokes-Einstein equation (Chp. 3, section 3.4).

4.2.2.3 Viscosity measurements

The steady-state viscosity of the microemulsions along one dilution line (corresponding to the 1:9 monostearin:Tween 20/ethanol ratio) was evaluated with a rheometer (C-VOR model, Malvern Instruments Ltd., Mississauga, Ontario, Canada) (Chp. 3, section 3.5). As discussed, this ratio was deemed most appropriate for further experimentation.

4.2.2.4 Differential scanning calorimetry (DSC)

DSC measurements were performed with a Perkin-Elmer Pyris-Diamond DSC (Markham, ON, Canada) (Chp. 3, section 3.6.). Heat/cool thermal analyses were conducted using the bulk monostearin and microemulsions. For the bulk monostearin, heating/cooling

rates of 5°C/min were used whereas for the microemulsion samples, heating rates of 5°C/min and cooling rates of 45°C/min were used to identify the presence of lipid in microemulsion. The 45°C/min cooling rate was used to imitate the super-cooling procedure which was later conducted to produce the SLNs.

4.3 Results and discussions

4.3.1 Pseudo-ternary phase behaviour - Effect of ethanol

The pseudo-ternary phase diagrams of the system W/M/T (water/monostearin/Tween 20) and W/M/T/E (water/monostearin/Tween 20/Ethanol) (Fig. 4-1 a and b, respectively) at 70°C resulted in large, isotropic microemulsion regions (the black area). The remainder of the phase diagram consisted of turbid, gel or multiphase regions, based on visual identification. Comparison of the microemulsion area in the two diagrams using imageJ image analysis software showed that addition of ethanol to the system at 1.5:1 ratio of Tween 20:ethanol increased the microemulsion area by 6.1% from 43.7% to 49.8%.

Effective microemulsion formation requires the presence of a water-soluble co-surfactant [60] (*e.g.*, short-chained alcohol) to reduce interfacial tension and increase the flexibility and fluidity of the interface, where it tends to position itself between the surfactant chains. Such partitioning modifies the solvent properties of both the dispersed and continuous microemulsion phases, lowers overall viscosity and prevents the formation of rigid structures (gels, liquid crystals and precipitates). Thus, the monophasic region within a ternary phase diagram can be increased in size [58,60-62,86,87].

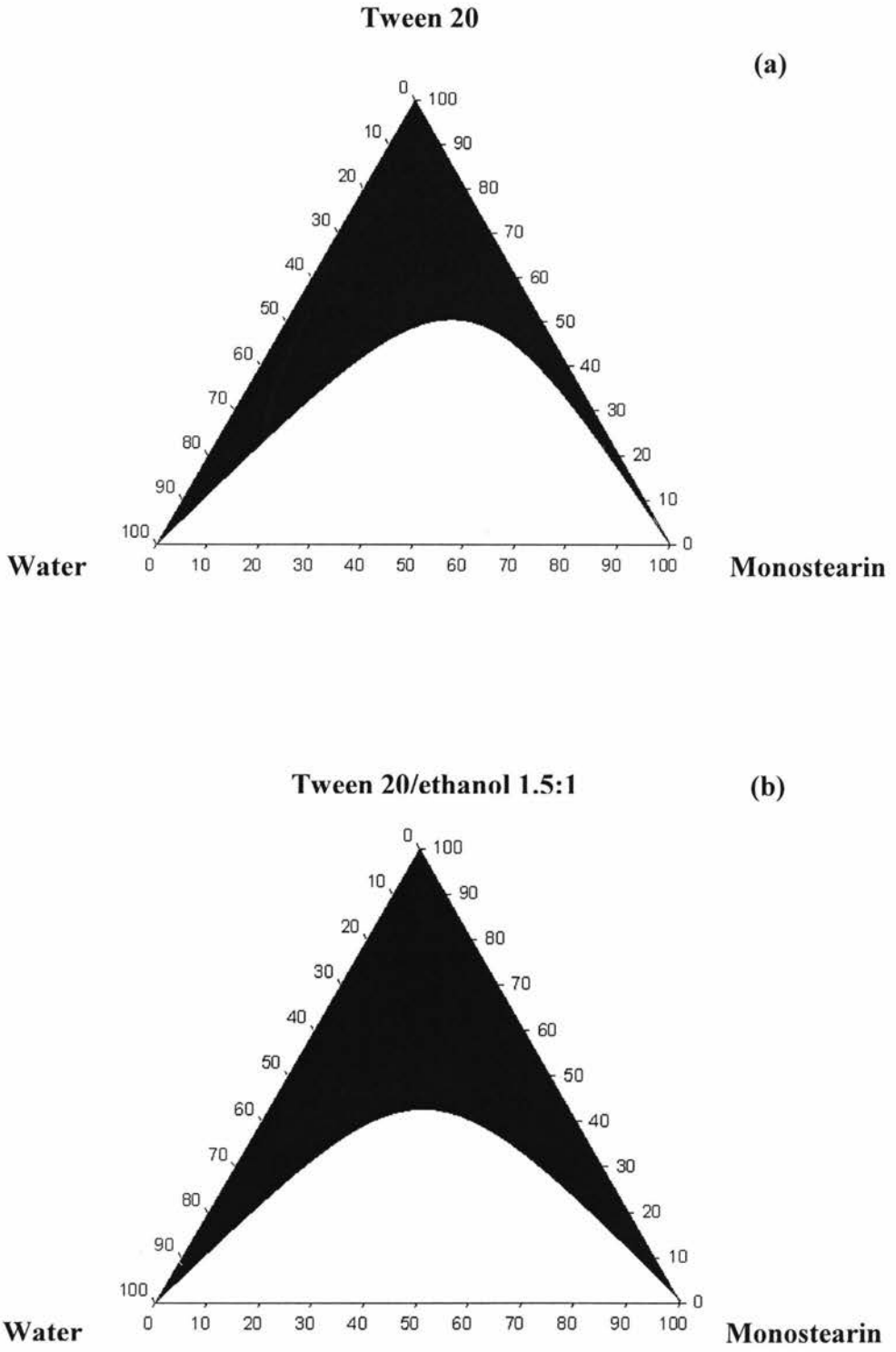

Figure 4-1: Pseudo-ternary phase diagrams at 70 °C for the (a) W/M/T system (microemulsion area (black) 43.7 %) and (b) W/M/T/E system (microemulsion area (black) 49.8 %).

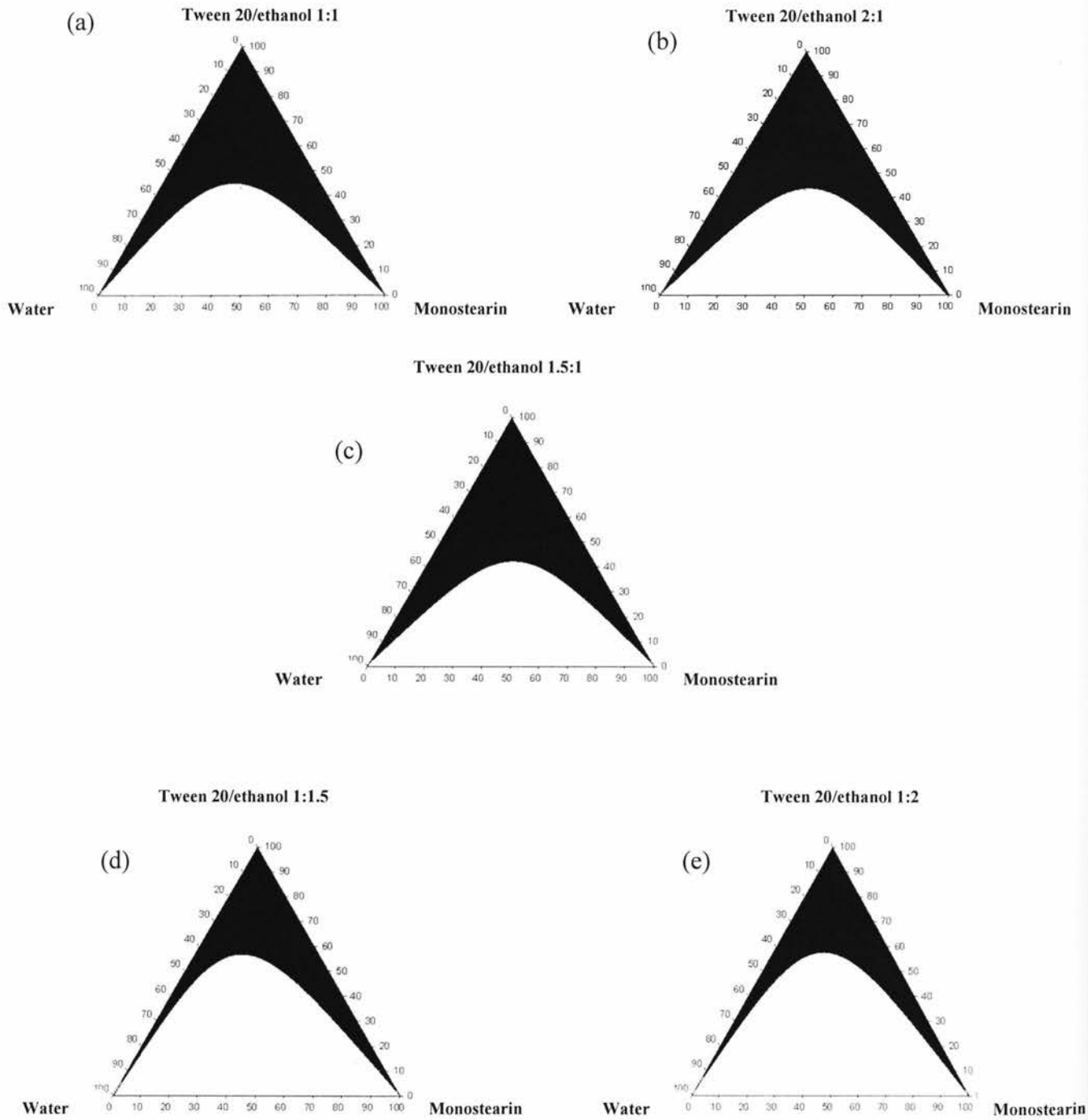

Figure 4-2: Pseudo-ternary diagrams for different Tween 20:ethanol ratios, which yielded different microemulsion areas (black area) (M.A) (a) 1:1 (M.A: 47.5 %) (b) 1.5:1 (M.A: 49.8 % (c) 2:1 (M.A: 49.9 %) (d) 1:1.5 (M.A: 47.7 %) (e) 1:2 (M.A: 47.4 %).

Co-surfactants also help to connect the O/W and W/O regions *via* a bicontinuous region, implying that all structural changes occurring in the monophasic region evolve without phase separation [58,88]. The effect of different ratios of Tween 20:ethanol (1:1, 1.5:1, 2:1, 1:1.5, and 1:2) on phase behaviour is shown in Fig 4-2. Fig 4-2 (b) and (c) show that there wasn't a major difference in microemulsion area between the 1.5:1 (49.8 %) and 2:1 (49.9 %) ratios, whereas the following ratios - 1:1, 1:1.5 and 1:2, decreased the microemulsion area to 47.5 %, 47.7 %, and 47.4 % respectively. For further experimentation, the 1.5:1 ratio was used.

4.3.2 Pseudo-ternary phase behaviour for the 10-90 dilution line

When a microemulsion region extends from the oil-rich region (W/O) to the water-rich region (O/W), the transition between these two often passes through a bicontinuous isotropic region [59,88]. The microemulsions that demonstrated this characteristic were those consisting of the 1:9 monostearin:Tween 20/ethanol ratio, with the Tween 20:ethanol ratio being 1.5:1 (Fig. 4-3). This set of microemulsions, which is hereafter referred to as the '10-90 dilution line', was used for further experimentation.

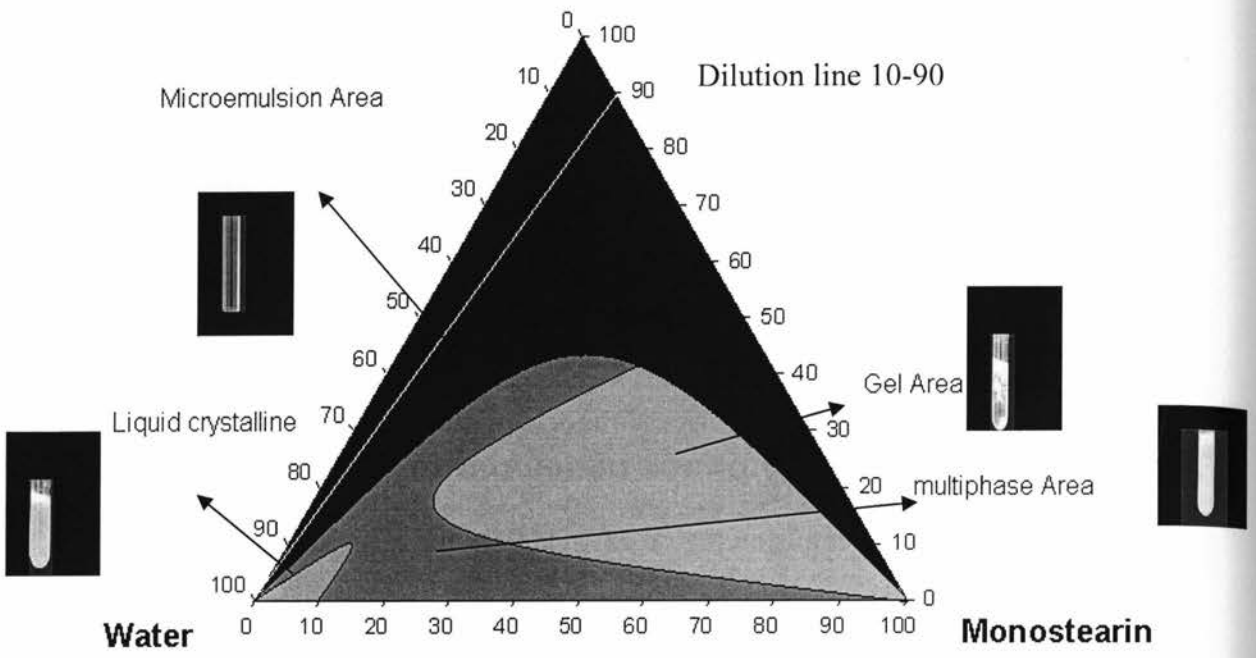

Figure 4-3: Pseudo-ternary diagram at 70 °C for the monostearin/Tween 20/ethanol/water system, showing the one phase microemulsion area (black), multiphasic area, gel area and liquid crystalline area (grey area).

4.4 Microemulsion phase characterisation

4.4.1 Particle size and polydispersity

The changes that occur during the transition from an oil-continuous phase to a water-continuous microemulsion were investigated by measuring the particle size and particle polydispersity with gradual dilution (Tab. 4-2). Samples from B-10 to B-90 represent the microemulsion samples with different water contents, where B-10 consists of 10 wt % water and B-90 consists of 90 wt % water (Tab. 4-1).

With a water content of 10 wt % to 40 wt %, particle size increased from about 438 nm to 539 nm (Tab. 4-2). With 10% water, the system preferentially formed water domains, even

though Tween 20 is highly hydrophilic. As the water content increased to 40%, W/O microemulsion structures remained, but water droplets swelled due to the extra water in the system causing an increase in droplet size. Polydispersity diminished from 0.1 with 10% water to 0.01 with 40% water, indicating more uniform particle sizes as water content increased.

Table 4-2: Particle size (nm) and polydispersity for microemulsion samples along dilution line 10-90. All data are means ± standard deviations (SD) for n = 3 replicates.

Sample	Particle size (nm) X ± SD	Polydispersity
B-10	438.8 ± 38.1	0.130 ± 0.005
B-20	446.1 ± 18.1	0.080 ± 0.007
B-30	481.0 ± 23.9	0.010 ± 0.007
B-40	539.0 ± 20.2	0.010 ± 0.005
B-50	348.6 ± 22.1	0.510 ± 0.005
B-60	0	0
B-70	0	0
B-80	17.5 ± 4.1	0.005 ± 0.000
B-90	17.6 ± 1.4	0.005 ± 0.000

With 50 wt % water, polydispersity substantially increased, suggesting that there were substantial changes in the microstructure of the aqueous domains. With 60 wt % and 70 wt % water, droplets were not detected, indicating a bicontinuous region. O/W microemulsion formation occurred with ≥ 80 wt % water. An average particle size of ~ 17 nm and a 0.005 polydispersity index suggested the presence of oil droplets.

The great difference between the size of the W/O microemulsion droplets (~ 450 nm) and O/W microemulsion droplets (~ 17 nm) may be due to the structure and aggregation behaviour of Tween 20. The high concentration of Tween 20 in the W/O emulsions combined with the very low water content led to a higher number of surfactant molecules per individual

water droplet [66]. Thermodynamically, though less than ideal, the limited contact afforded by the small water content was still more favourable than micelle formation in the absence of any moisture.

Conversely, in the O/W region the microemulsion domain size was much smaller due to the structure of Tween 20, with its lipophilic tails oriented towards the oil phase and thus less steric repulsion [66,77]

4.4.2 Conductance

Conductance (Fig. 4-4) increased continuously with an increase in water content. The low conductance in the W/O region was an indication of the low water content. High conductance values (above 60 wt% water content) along the 10-90 dilution line suggested that the system evolved from an oil-continuous to a water-continuous environment, as has been observed elsewhere [66,88].

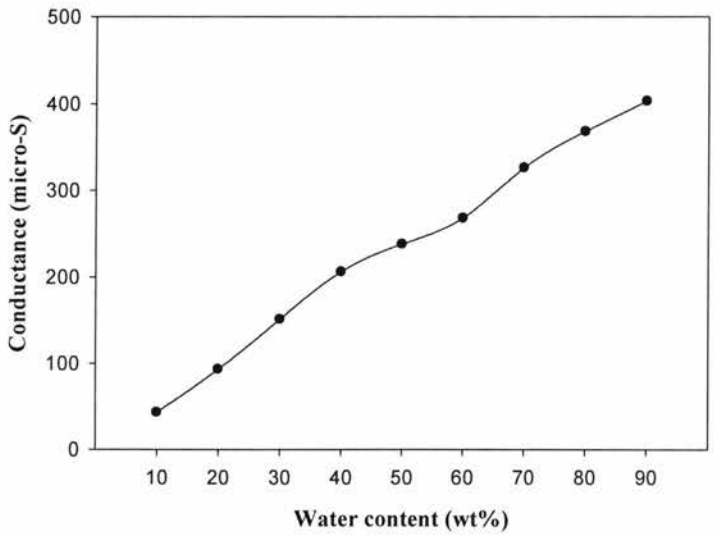

Figure 4-4 Electrical conductance (μS) of the monostearin/Tween 20/ethanol/water as function of water content along dilution line 10-90. All data are means ± standard deviation for n = 3 replicates. (Standard deviation bars are very small and are not shown in the graph.)

4.4.3 Viscosity

At a water content between 10 and 50 % (w/w), there was little change in viscosity (Fig. 4-5). With higher water contents ($\geq$ 60 wt %), the viscosity of the microemulsions decreased sharply. Up to 50 wt %, the lack of chance in viscosity was consistent with particle size data where oil-continuous domains dominated. The reduction in viscosity at higher water contents may be attributed to the transition to bicontinuous structures and subsequent water-continuous region.

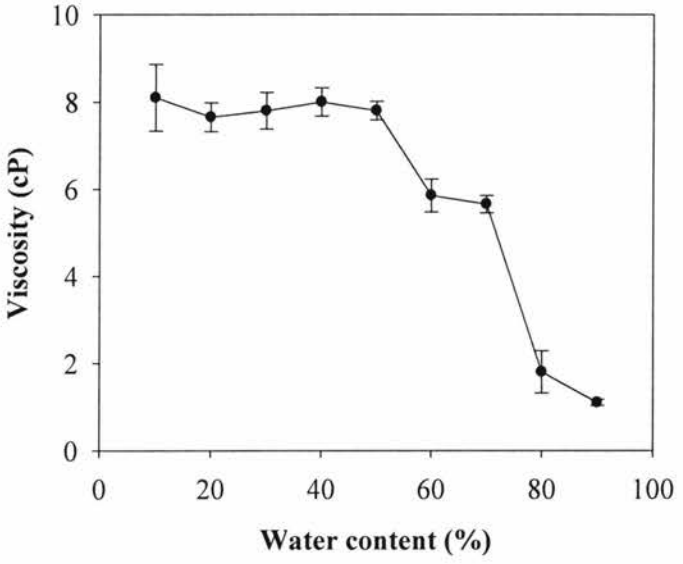

Figure 4-5: Viscosity (η) of the monostearin/Tween 20/ethanol/water system as function of water content along dilution line 10-90 at 70 °C. All data are means ± standard deviation for n = 3 replicates.

4.4.4 Microemulsion thermal behaviour

The thermal behaviour of select O/W microemulsions was initially investigated using DSC using heating and cooling rates of 5°C/min [89]. However, this cooling rate did not show any thermal events for the microemulsions between 80 and 10 °C, thus a cooling rate of

45°C/min (similar to the SLN quenching protocol) was used to induce measurable crystallisation (Chp. 5). The results were compared with that of bulk monostearin (Fig 4-6). Within the microemulsions, the thermal events were due to monostearin as this was the only component that underwent a liquid-to-solid transition in this temperature range (Fig. 4-6, a). Bulk monostearin melted at 71.76 ± 0.05 °C and crystallised at 67.02 ± 0.14 °C, which was in agreement with the literature [44] . Monostearin within microemulsions consisting of 80 wt % water, 18 wt % Tween 20/ethanol and 2 wt % monostearin melted at 45.80 ± 2.34 °C and crystallised at 35.80 ± 1.72°C (Fig. 4-6, b).

Differences in melting and crystallisation for bulk vs. microemulsion monostearin were due to its compartmentilisation within nano-sized domains [90-94]. The relationship between particle size and crystallisation temperature has been discussed for different lipids [90-93]. For example, the crystallization temperature of bulk tristearin, tripalmitin, trimyristin and trilaurin (51°C, 42°C, 28°C and 11°C, respectively) can be delayed by ~20°C, when these are dispersed into droplets [44].

The melting enthalpy of bulk monostearin was 98.37 ± 4.64 J g^{-1} whereas it was 74.05 ± 0.87 J g^{-1} for the monostearin particles in the microemulsion. The crystallisation enthalpy also decreased as it was 91.57 ± 7.53 J g^{-1} for bulk monostearin and 77.94 ± 3.13 J g^{-1} for monostearin particles in the microemulsion.

Statistical analysis showed that melting and crystallisation temperatures and also melting and crystallisation enthalpy were statistically significantly different for bulk monostearin and monostearin in microemulsion ($p > 0.05$).

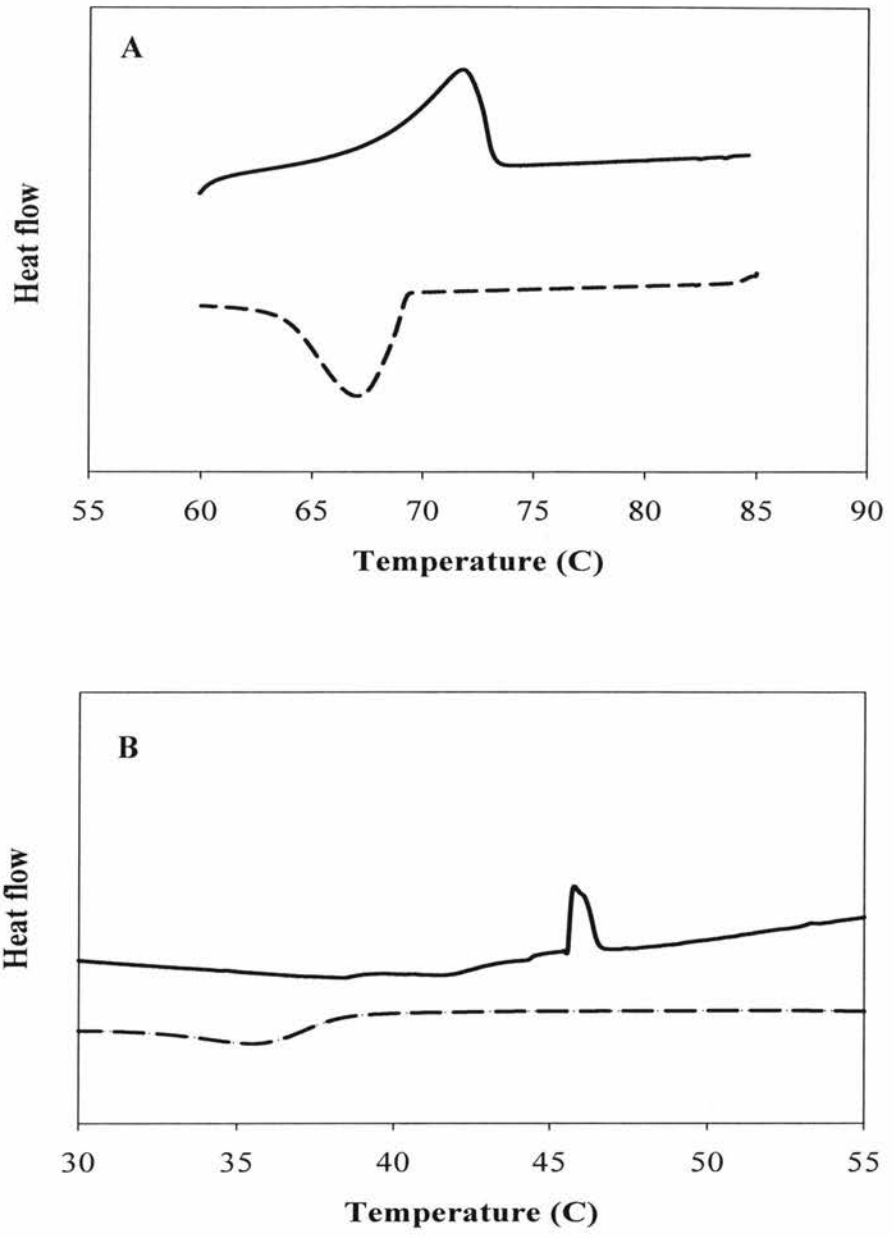

Figure 4-6: DSC heating and cooling (5˚C/min) of bulk monostearin (A) and heating (5˚C/min) and cooling (45˚C/min) of a microemulsion consisting of 80% water, 18% Tween 20/ethanol, and 2% monostearin (B)

4.5 Conclusions

Microemulsions based on food-grade materials were developed. The phase behaviour and properties of four-component microemulsions were investigated using DLS to measure particle size, polydispersity and conductance. Rheometry was used to measure viscosity, and DSC was used to identify the thermal behaviour of the oil used in the microemulsion system. The results of these analyses permitted the elucidation of the structural evolution and transitions of these microemulsions from aqueous-poor to aqueous-rich regions.

Chapter 5

SLN development & characterisation

5.1 Introduction

Solid lipid nano-particles (SLNs) are particles made from solid lipids (*i.e.*, lipids solid at room temperature and also at body temperature). The lipids used can be highly purified triglycerides, complex glyceride mixtures or even waxes [43]. There has been extensive use of SLNs in pharmaceuticals research as drug carriers [43,51,69,70,79,80,96-98]. For applications in the food industry, SLNs have been studied as vehicles for the controlled delivery of flavours or nutraceuticals.

Different approaches exist for the production of finely-dispersed lipid nanoparticles, including high shear homogenisation and ultrasound [97]. Both methods are widespread and easy to use. High pressure homogenisation (HPH) can be performed at elevated temperatures (hot HPH technique) or below room temperature (cold HPH technique). The influence of homogeniser type, applied pressure, homogenisation cycles and temperature on particle size distribution has been studied [43]. Both HPH techniques are suitable for processing lipid concentrations of up to 40 wt % and generally yield narrow particle size distributions (polydispersity index < 0.2).

Different groups have attempted the production of SLNs via precipitation using solvent emulsification-evaporation [43]. In this method, the lipid is dissolved in a water-immiscible organic solvent (*e.g.* cyclohexane, toluene, chloroform), which is then emulsified in an aqueous phase before evaporation of the solvent under reduced pressure. Upon evaporation of the solvent, the lipid precipitates forming SLNs. An important advantage of this method is the

avoidance of heat during the preparation, which is important mainly when particles are loaded with heat-sensitive materials (*e.g.*, drugs) whereas a clear disadvantage is the use of organic solvents [43,97].

Gasco *et al.* (1993) developed SLNs based on the dilution of microemulsions. Later, this method was adapted or modified by others [45]. In their approach, microemulsions were made by stirring an optically transparent mixture at about 70 °C, typically composed of a low melting fatty acid (*e.g.* stearic acid), an emulsifier (*e.g.* polysorbate 20, polysorbate 60, soy phosphatidylcholine, taurodeoxycholic acid salt), co-emulsifiers (*e.g.* butanol, sodium monooctylphosphate) and water. The hot microemulsion was then dispersed in cold water (2-3 °C) at ratios of 1:25 to 1:50, with stirring [45,99] to yield the SLNs. Excess water was removed by ultrafiltration or by lyophilisation in order to increase the particle concentration.

The scale-up of SLN production via microemulsions was studied by Marengo *et al.* in 2000 [52]. In their study, experimental factors such as dispersion device, temperature, and volume of dispersing water were optimised to maximise SLN yield. They compared micropipettes and needles as means to disperse warm O/W microemulsions into cold water. The former resulted in particles 55 nm in size whereas the latter produced smaller particles (~ 35 nm). Different volumes of cold water (2-4 °C) from 20 ml to 230 ml were used to super-cool 25 ml of warm microemulsion, with the best results achieved with the highest volume of dispersing water (230 ml cold water for 25 ml warm microemulsion).

5.2 Experimental

5.2.1 Materials

These are described in (Chp. 3, section 3.1 and 3.2).

5.2.2 Methods

Warm (70 °C) O/W microemulsions with an average particle size of 15 nm were prepared (Chp. 3, section 3.1) and the SLNs were subsequently produced (Chp. 3 section 3.2). The influence of adding lecithin to the warm microemulsion in order to stabilise monostearin nanoparticles was investigated by evaluating particle size, polydispersity index and conductance. In addition, DSC was conducted on the lecithin-treated O/W microemulsions to study its effect on crystallisation, if any. Particle size, polydispersity index and ζ-potential were measured using DLS. Atomic force microscopy was used to confirm the existence of SLNs in the nm range. DSC results were used to tailor the quench-cooling protocol.

5.2.2.1 Dynamic light scattering

A Brookhaven 90Plus/BI-MAS (Brookhaven Instruments Corporation, Holtsville, New York, USA) was used to measure SLN particle size (nm), polydispersity and ζ-potential (mV) at 25 °C (Chp. 3, section 3.4).

5.2.2.2 Atomic force microscopy

Air-dried SLN samples mounted on a mica slide were imaged at ambient temperature (Chp. 3, section 3.10).

5.2.2.3 Differential scanning calorimetry

DSC measurements were performed with a Perkin-Elmer Pyris Diamond DSC (Markham, ON, Canada) (Chp. 3, section 3.6) for bulk and microemulsified monostearin. Samples were ramped from 25 to 80 °C at heating rate of 5 °C/min and a cooling rate of 45 °C/min to simulate the super-cooling necessary to form the SLNs.

5.3 Results and discussions

5.3.1 Optimised microemulsion formulation

To develop the SLNs, warm microemulsions (70 °C) were quench-cooled with cold water (4 °C) while stirring. According to earlier DSC results (Chp. 4, Section 4.4.4), microemulsified monostearin solidified at ~35 °C. Extensive aggregation of the prepared SLN was visible after 5 h, likely due to particle-particle coalescence and growth. High-PC lecithin (> 97 %) was used to alter the ionic environment surrounding the SLNs (Chp. 2, section 2.4.6). Different amounts of lecithin [0.2, 0.5, 1.0 and 2.0 wt %] were added to the microemulsions along dilution line 10-90. Samples with 0.5 wt % lecithin stayed clear at 70°C for one month. A higher amount of lecithin (1 wt %) resulted in a turbid solution, indicative of insolubility or phase separation whereas a lower amount (0.2 wt % lecithin) did not enhance stability.

5.3.2 Characterisation of the optimised microemulsions

Table 5-1 shows the particle size and polydispersity index of the microemulsions with 0.5 wt % added lecithin, along dilution line 10-90. In the W/O region, the particle size ranged from ~ 530 nm for microemulsions with 10 wt % water to about 350 nm for samples with 40 wt % water. At 50 wt % and 60 wt% water, the droplet size was ~ 100-200 nm. However, the polydispersity index increased from 0.005 with 50 wt % to 0.886 with 60 wt %. With 70 wt % water, droplets were not detected, indicative of bicontinuous structures. Further dilution to 80 wt % and 90 wt % water led to the formation of oil domains. The particle size was 10-15 nm with low polydispersity (0.005). Compared to the microemulsions *sans* lecithin, the bicontinuous region became smaller in the presence of lecithin.

Table 5-1: DLS of microemulsions treated with 0.5% (w/w) lecithin

Sample	Particle size (nm) $X \pm \sigma$	Polydispersity
B-10	503.3 ± 21.8	0.180 ± 0.007
B-20	480.4 ± 33.1	0.130 ± 0.007
B-30	435.5 ± 24.8	0.005 ± 0.005
B-40	350.1 ± 21.0	0.005 ± 0.005
B-50	102.8 ± 19.1	0.005 ± 0.005
B-60	171.8 ± 22.5	0.880 ± 0.010
B-70	0	0
B-80	15.7 ± 4.8	0.005 ± 0.000
B-90	15.6 ± 1.2	0.005 ± 0.000

Particle sizes in the microemulsions with and without lecithin were not statistically significantly different with 10-30 wt % and 80-90 wt % water ($p > 0.05$). Conversely, statistically significantly differences were observed in the microemulsions with 40-60 wt % water ($p < 0.05$).

There was a continuous increase in conductance (Fig. 5-1) with an increase in water content, as previously explained (Chp. 4, section 4.4.2). However, conductance values with lecithin were higher than without lecithin, which is charged.

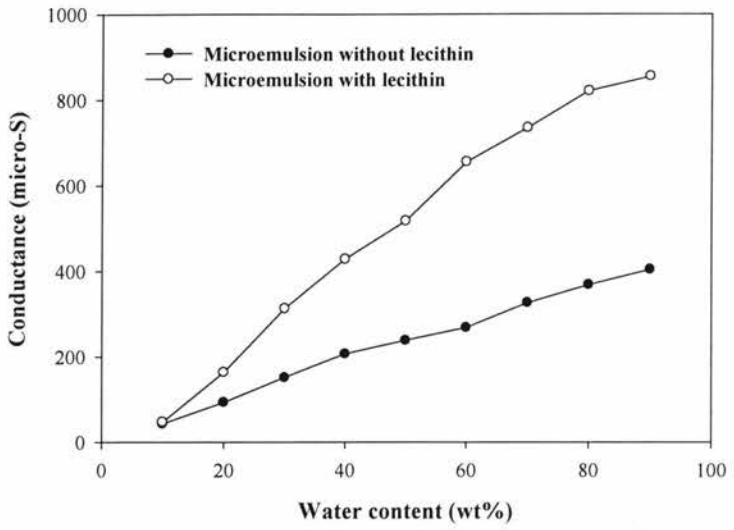

Figure 5-1: Influence of added lecithin (0.5% w/w) on microemulsion conductance (μS) as a function of water content along dilution line 10-90. All data are means ± standard deviations for n = 3 replicates. (Standard deviation bars are very small and is not shown in the graph.)

5.3.3 Thermal analysis

Fig. 5-2 shows the DSC heating and cooling curves for bulk monostearin (Fig 5-2A), the microemulsion without lecithin (Fig. 5-2B) and microemulsion treated with lecithin (Fig. 5-2C). The melting point of nano-sized monostearin in the untreated microemulsion was 45.80 ± 2.34 °C whereas in bulk monostearin, it was 71.76 ± 0.05 °C. The ~ 26 °C difference can be explained by the compartmentilisation of the monostearin into small microemulsion domains.

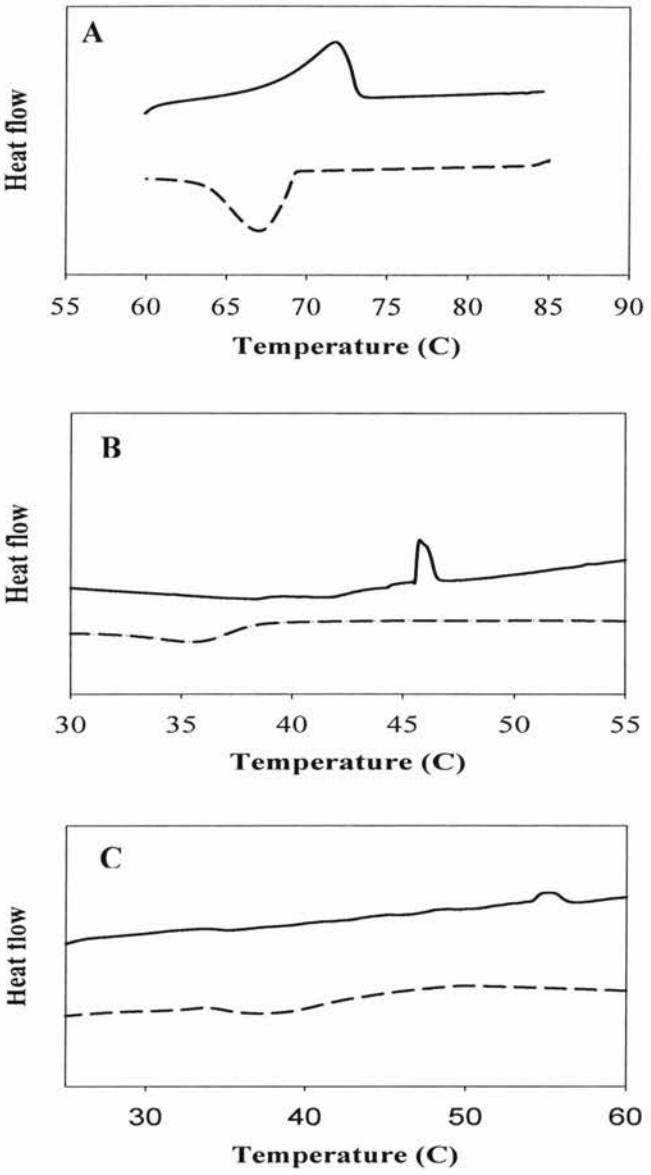

Figure 5-2: DSC heating and cooling curves of (A) bulk monostearin; (B) the 'untreated' microemulsion; and (C) the treated microemulsion (straight line: melting and dashed line: crystallisation)

For the microemulsions treated with 0.5% lecithin, the melting point rose to 55.01 ± 4.02 °C, likely due to the increase in crystal size noted in the presence of lecithin. Similar trends have been observed in the literature with other fatty materials [91,92].

The peak crystallisation temperature of the nanoparticles in the untreated microemulsions was 35.80 ± 1.72 °C, which is ~ 30 °C less than in the bulk (67.02 ± 0.14 °C). The crystallisation temperature peak in the microemulsions with lecithin occurred at 38.07 ± 2.18 °C, which is almost the same as the untreated microemulsions. However, during the crystallisation of the SLNs with quench cooling, crystallisation took longer in the microemulsions treated with lecithin (30-45 min) compared to 15-30 min for the untreated microemulsions.

Table 5-2 summarizes the DSC results for bulk and microemulsified monostearin. Addition of lecithin (0.5%) to the microemulsion increased the particle size to ~120 nm (see DLS section).

Table 5-2: DSC results for bulk monostearin and microemulsion monostearin with and without lecithin. All data are means ± standard deviations for n = 3 replicates.

Monostearin	Particle size (nm)	T_m (°C)	ΔH_m (Jg^{-1})	T_c (°C)	ΔH_c (Jg^{-1})
Bulk	--	71.76 ± 0.05	98.37 ± 4.64	67.02 ± 0.14	91.57 ± 7.53
ME (2%)	17.50 ± 4.10	45.80 ± 2.34	74.05 ± 0.87	35.80 ± 1.72	77.94 ± 3.13
ME+Lec (2%)	120.42± 18.3	55.01 ± 4.02	78.55 ± 3.96	38.07 ± 2.18	80.52 ± 4.22

The melting enthalpy of the lecithin-treated microemulsions was 78.55 ± 3.96 J g^{-1}, compared to untreated microemulsions (74.05 ± 0.87 J g^{-1}) and 98.37 ± 4.64 J g^{-1} for bulk monostearin. The crystallisation enthalpy decreased to 80.52 ± 4.22 J g^{-1} for the lecithin-treated microemulsions and 77.94 ± 3.13 J g^{-1} for untreated microemulsions compared to 91.57 ± 7.53 J g^{-1} for the bulk monostearin.

The suppression of melting and crystallisation temperatures has been discussed extensively in the literature [90-94]. Models based on the Thomson equation (equation 5-1)

modified for crystalline materials are often used to describe the relationship between particle size and melting temperature [91]:

$$-\frac{T_0 - T}{T_0} \approx \ln\frac{T}{T_0} = -\frac{2\gamma_{sl}V_s}{r\Delta H_{fus}} \qquad (5\text{-}1)$$

where T is the melting temperature of a particle with radius r, T_0 is the melting temperature of the bulk material, γ_{sl} is the interfacial tension at the solid-liquid interface, V_s is the specific volume of the solid, and ΔH_{fus} is the specific heat of fusion. From this equation, it is expected that the melting temperature and enthalpy of colloidal substances will decrease with a decrease in particle size.

5.3.4 Dynamic light scattering

The particle size, polydispersity, and ζ-potential of the monostearin particles generated via quench-cooled microemulsions were measured using DLS (Table 5-3). A particle size of 120 nm with 0.15 polydispersity index was measured immediately following preparation (day 0).

Table 5-3: Particle size (nm), polydispersity, and ζ-potential measurements for SLN samples (day 0). All data are means ± standard deviations for n = 3 replicates.

Particle size $\mathbf{X \pm \sigma}$	**Polydispersity** $\mathbf{X \pm \sigma}$	**ζ-potential** $\mathbf{X \pm \sigma}$
120.4 ± 18.3	0.15 ± 0.08	-40.0 ± 5.2

The ζ-potential of the SLN solution was ~ -40 mV. ζ-potentials ~ |30| mV are not sufficiently high to stabilise dispersions solely by electrostatic repulsion, whereas optimum stabilisation is achieved with >|60| mV. Potentials between |5| and |15| mV lead to limited flocculation and values between |5| and |3| mV result in maximum flocculation [13]. Thus,

particle aggregation was likely to occur for charged particles (ζ-potential = -40 mV), due to insufficient electrical charge to prevent aggregation.

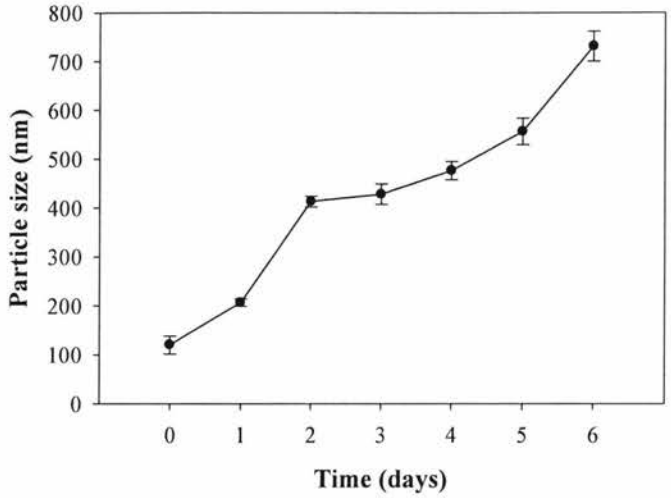

Figure 5-3: Monostearin nanoparticle growth profile from day 0 to day 6. All data are means ± standard deviations for n = 3 replications.

The nanoparticle crystal growth profile was studied for one week following preparation. Particle size increased in size from the first day onwards (Fig. 5-3), increasing to 731 nm by the end of the week.

AFM was used to image the SLNs and confirm the diameter measured with DLS (120 nm). With AFM, SLNs with diameters of 115.62 ± 28.46 nm were measured (Fig 5-4), in agreement with DLS results. There was no statistically significant difference between particle size measurements with DLS and AFM ($p > 0.05$).

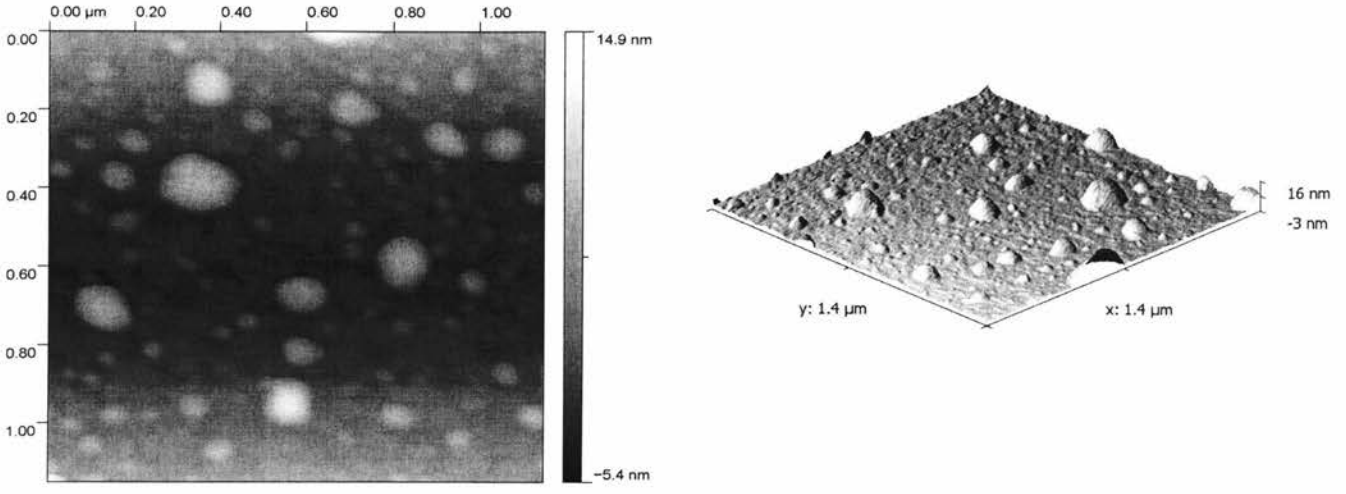

Figure 5-4: AFM height images of monostearin SLNs following preparation.

The AFM image revealed that the morphology of the monostearin particles was elongated.

5.3.5 SLN harvesting

The prepared SLNs were centrifuged for 2 × 30 min at 3500 rpm (IEC-Centra-CL2 centrifuge, International Equipment Company, MA. USA), as explained in Chp. 3, Section 3.2. The obtained SLNs were diluted with water at 1:50 ratio and measured by DLS to check the particle size after centrifugation. As a result of centrifugation, the monostearin nanoparticles increased in size to 644.33 ± 42.37 nm.

5.4 Conclusions

Lipid nanoparticles were prepared using an O/W microemulsion template and stabilised with lecithin. The addition of lecithin did affect the phase behaviour of the microemulsion by reducing the size of the bicontinuous region. SLNs ~120 nm in diameter with a unimodal distribution were obtained by super-cooling the microemulsion at a 1:10 ratio in cold water (4 °C). The monostearin nanoparticles started to increase in size immediately following

preparation. Centrifugation resulted in an increase in SLN size, which grew to ~650 nm. These particles were used for W/O emulsion stabilisation described later.

Chapter 6

Pickering stabilisation of W/O emulsions

6.1 Introduction

Pickering emulsions are composed of droplets of one immiscible liquid dispersed in another liquid and are stabilised by interfacially-active solid particles (Pickering, 1907). Such systems are often encountered in the recovery, separation, and cleaning of crude oil, in cosmetic preparations, and in wastewater treatment [100].

Solid particles adsorbed at an interface can provide long-term kinetic stability to emulsions and foams by providing a steric barrier to coalescence [101]. The effectiveness of such particles is often related to the particle attachment energy and morphology properties of the particles (chp. 2 section 2-1). The particle attachment energy at an interface for an ideal spherical particle is:

$$E = \pi\alpha^2 \gamma \, (1 \pm \cos\theta)^2 \qquad (6\text{-}1)$$

where α is the particle radius, γ is the oil-water interfacial tension, and θ is the contact angle measured across the aqueous phase. When measured through the aqueous phase, the contact angle formed with hydrophilic particles is $< 90^\circ$, leading to O/W emulsion stabilisation and $> 90^\circ$ for hydrophobic particles. In this study, solid lipid (monostearin) nanoparticles (SLNs) with an average diameter of ~ 120 nm were used to stabilise W/O emulsions. SLNs were harvested the day of production and used immediately as centrifugation and homogenisation affected the particle size.

6.2 Experimental section

6.2.1 Materials

For the emulsion preparation, reverse osmosis water (AMTROL Inc., West Warwick, RI, USA) was used. Light mineral oil (>99% purity, Fisher Scientific, Ottawa, ON, Canada) was used as the oil phase. The solid monostearin nanoparticles described in Chp. 5 were used as surface-active solid particles. The fluorescent stains Rhodamine B (Fisher Scientific, Ottawa, Ontario, Canada) and fluorol yellow 088 (Sigma-Aldrich, Oakville, Ontario, Canada) were used at 0.01% (w/w) in the aqueous and oil phases, respectively.

6.2.2 Methods

The prepared SLNs were centrifuged for 30 minutes at 6000 rpm. The SLNs sediments were collected and used for the W/O emulsions.

6.2.2.1 W/O emulsion preparation

All emulsions consisted of 20% water, SLNs at different concentrations [0.5, 1, 1.5, and 2 wt %)] and light mineral oil as the oil phase (78-79.5 wt %). The emulsions were prepared using an Omni-Mixer homogeniser (London Scientific, London, Ontario, Canada), which had a micro-attachment containing a blade-type impeller (total cell volume = 5 ml). Evaluation of homogenisation time was performed on emulsions with 1.5% SLNs for 2, 5 and 10 minutes to study the impact of homogenisation time on the water droplet size and stability. In the end, emulsions were prepared by mixing at ~5000 rpm for 1 minute to pre-blend followed by 2 minutes at ~27,000 rpm to homogenise.

6.2.2.2 Contact angle measurements

Monostearin was melted at ~75 °C while stirring and poured into aluminium weigh boats at room temperature and allowed to crystallise for ~3 h. The solidified disks were then cut into ~1 cm cubes and placed in spectrophotometer cuvettes, with the smooth bottom side facing upwards. Cuvettes were then filled with light mineral oil. A small droplet (D ~ 1 mm) of water was then injected onto the surface of the solid fat from a needle (gauge 22, Fisher Scientific, 0.711 mm nominal outer diameter and 0.394 mm nominal inner diameter), using a 10 ml syringe using a programmable syringe pump (kd Scientific, Markham, ON, Canada) at 0.1 ml/min. Images of the water droplet were captured with a Teli CCD camera with macro lens assembly and IDS Falcon/Eagle Framegrabber (DataPhysics Instrument GmbH, Filderstadt, Germany) for up to 5 d. Image analysis to determine contact angle of the droplet against the solid surface was performed using SCA 20 version 2.1.5 build 16.

6.2.2.3 Pulsed nuclear magnetic resonance (pNMR)

A Bruker Minispec Mq pulsed (pNMR) unit (Bruker Canada, Milton, Ontario, Canada) equipped with a pulsed field gradient unit was used to characterise the W/O emulsion droplet size distribution (DSD) and solid fat content (SFC). Emulsion samples were pipetted into NMR tubes (1 cm o.d. and L = 15 cm) for NMR droplet size analysis (1 cm height samples) and SFC respectively (4 cm height samples). DSD samples were analysed within 1 h of preparation (day 0) and at days 1, 2, 4, 7, 10 and 14.

6.2.2.4 Confocal laser scanning microscopy

A confocal laser scanning microscope was used in fluorescence and polarised light mode to evaluate the emulsion and SLN morphology as well as their spatial arrangement. A Zeiss Axioplan-2 microscope equipped with a LSM 510 confocal module and the associated

software (version 3.2; Zeiss Instruments, Toronto, ON, Canada) was used with a 63x Achroplan water-immersion objective. Emulsion samples for microscopy analysis were prepared as described in section 6.2.2.1, except that the fluorescent dyes Rhodamine B (Fisher Scientific, Ottawa, ON, Canada) and fluorol yellow 088 (Sigma-Aldrich, Oakville, ON, Canada) were added to the water and oil phases, respectively at 0.01% (w/w). Rhodamine B was excited at 543 nm and fluorol yellow at 488 nm with the emitted light passing through an LP 505 filter for detection. Previous studies in our lab had shown that at these concentrations, these stains did not influence emulsion properties (i.e., mean droplet size and DSD). All data are shown as means ± standard deviations for n = 3 replicates.

6.3 Results and discussions

6.3.1 Adsorption to interface

For particles to stabilise emulsion droplets, they should be located at the interface, but more within the continuous phase. In the case of a W/O emulsion, the contact angle of a water droplet against a solid body should be > 90°, when viewed through the water phase (Fig. 6-1).

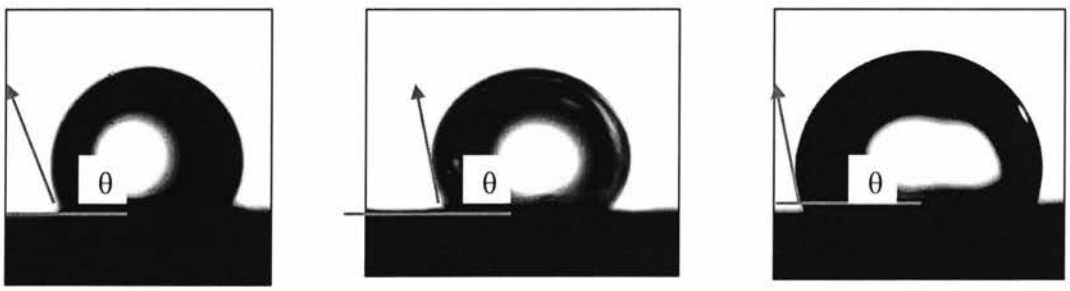

Day 0, θ = 127.8 ° ± 1.8	Day 1, θ = 115.9 °± 2.3	Day 2, θ = 114.7 ° ± 1.2

Figure 6-1: Contact angle measurements of a water drop on a solid monostearin mass in mineral oil. All data are means ± standard deviations for n=3 replicates, with the left and right hand contact angles averaged for each replicate.

The dark base in the above images is the solidified monostearin upon which sits the water droplet surrounded by mineral oil. The measured contact angle on day 0 was ~128°, after which it decreased for 3 d until reaching a constant value (θ = 114.7 ± 1.2°). These results demonstrated that monostearin is surface-active and preferentially partitions towards the water-mineral oil interface during emulsification. A contact angle > 90° shows that monostearin is lipophilic and will tend to stabilise W/O emulsions.

The energy of attachment of a particle to a fluid-fluid interface is related not only to the contact angle, but also to the interfacial tension (γ_{ow}) [101,102]. The interfacial tension of water and mineral oil was determined using a ASTM method D971, with the DuNouy ring method (Fisher surface tensiometer Model 21, Fisher Scientific, Nepean, ON, Canada). The measured mineral oil-water interfacial tension was 0.035 ± 0.001 N m^{-1} (literature value: 0.035 N m^{-1}) [102] . Assuming that the particles are small enough (D < ~ 1 μm), the effect of gravity will be negligible, and the energy (E) required to remove a particle of radius α from the interface will be [102]:

$$E = \pi\alpha^2 \gamma_{ow} (1 \pm cos\theta)^2 \qquad (6\text{-}2)$$

The sign inside the bracket is negative for displacement into the water phase, and positive for displacement into oil. The displacement energy for the monostearin into the aqueous phase was 5.7 x 10^6 kT. The same equation has been used [9,27,38] to calculate the removal energy of 10 nm silica particles in a toluene-water mixture, where the particles were held at the interface with E ~ 2750 kT. In this study, had the monostearin crystals measured only 10 nm, the displacement energy would have yielded similar values (~5400 kT). The very high attachment energy of the SLNs to the oil-water interface supports the supposition that the particles were effectively adsorbed to the interface.

6.3.2 Sedimentation

Emulsions used for evaluating sedimentation consisted of 20 wt %) water, SLNs (0.50 ± 0.12, 1.00 ± 0.08, 1.50 ± 0.07, 2.00 ± 0.10 wt %) and 78-79.5 wt % mineral oil. Emulsions with 1.5 wt % SLNs were used to optimise the homogenisation protocol. These samples were homogenised for 2, 5 or 10 min and the effect of homogenisation duration was studied by measuring sedimentation kinetics, DSDs and microstructure. Figure 6.2 shows the effect of homogenisation time on sedimentation over 14 d at room temperature. The grey regions consisted of emulsified water droplets and dispersed solid fat crystals (white) whereas the oil continuous phase shows in background. At higher solids level [1.5% and 2% (w/w) SLNs; Figs 6-2 c-2 min and d-2 min], emulsions were more stable against sedimentation than those with 0.5, and 1% (w/w) SLNs [Figs 6-2 a-2min and b-2 min]. This was somewhat associated with their resistance to coalescence, as discussed later.

Emulsions with 0.5% (w/w) SLNs were orange (here shows as dark grey), which indicated the presence of free water stained with Rhodamine B. The oil phase separated almost immediately after 2 min of homogenisation (Fig 6-2 a-2min). The supernatant oil at day 0 comprised ~70% of the emulsion height and ~77% at day 14.

Emulsions with 1 wt% SLNs were light orange, which indicated a lesser amount of free water than the emulsions with 0.5 wt % SLN (Fig 6-2 b-2min). However, some channelling was observed, which may have been due to air bubble incorporation and/or the breakage of the emulsion where interparticle interactions (i.e., between crystals) were weakest. On day 0, 4 separate layers were present in the emulsion whereas on day 14, the existence of only 2 layers indicated macroscopic phase separation.

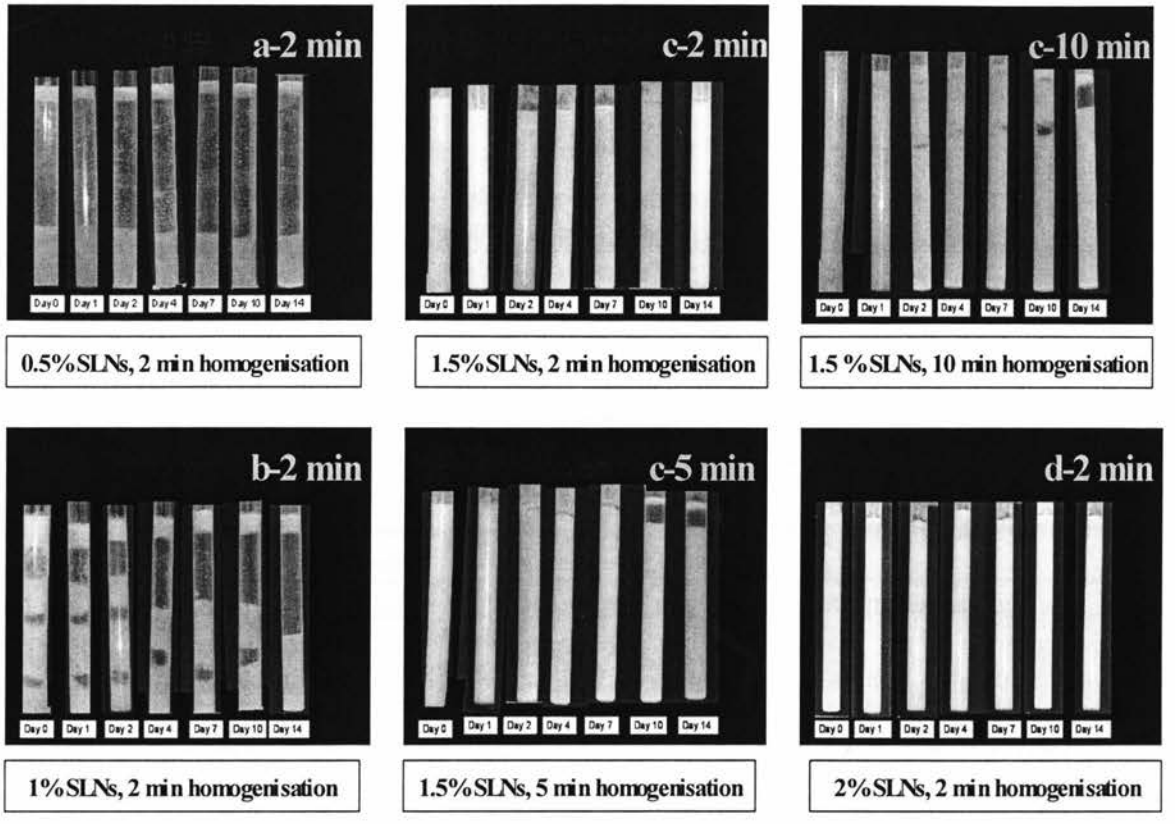

Figure 6-2: Emulsion sedimentation for samples prepared under the following conditions: a-2 min (0.5 wt% SLN and 2 min homogenisation), b-2 min (1 wt% SLN and 2 min homogenisation), c-2 min, c-5 min, c-10 min (1.5 wt% SLN and 2, 5, 10 min homogenisation) and d-2min (2 wt% SLN and 2 min homogenisation).

The top cream-like layer that accounted for ~16% of the total volume on day 0 and ~9% on day 14 was probably a foam-like structure with entrapped air bubbles. By day 4, the sediment had increased to ~23% of sample height from ~14% at day 0. The separated oil phase for day 0 was ~24% and this value increased to ~53% of sample height at day 14.

Emulsions with 1.5 wt % SLNs, showed an enhanced resistance to sedimentation and creaming (Fig 6-2 c-2 min). Limited oil separation was observed at days 7 and 14. Longer homogenisation times (Fig. 6-2 c-5 min and c-10 min) did not improve the stability of emulsions with the same level of SLNs, as phase separation was observed for both emulsions. Thus, the increased shear due to longer homogenisation times prevented effective emulsion

stabilisation, perhaps due to the physical breakdown of the SLNs. Emulsions with 2 wt % SLNs and 2 minutes homogenisation did not show any macroscopic phase separation over 14 days (Fig 6-2 d-2min).

6.3.3 Evolution in droplet size via NMR

NMR measurements were conducted on days 0, 1, 2, 4, 7, 10, and 14 following emulsion preparation. The results reported below include the volume-weighted mean droplet diameter (d_{33}), emulsion polydispersity (σ) and free water (Tab. 6-1). The emulsions that were not measurable with NMR were deemed unstable and not characterized.

As per the sedimentation results (section 6.3.2), emulsions with 0.5% and 1% (w/w) SLNs were unstable against coalescence, as further described in the microscopy section below. As a general rule, a 0 value for σ indicates an unstable system. The presence of SLNs at 1.5% and 2% (w/w) in the emulsions homogenised 2 min (c-2 and d-2, respectively) resulted in detectable emulsions. However, emulsions with 1.5% (w/w) homogenised 5 and 10 min were not stable against coalescence.

Table 6-1: d_{33}, σ and free water values for emulsions with 0.5 wt% (a-2min), 1 wt% (b-2min), 1.5 wt% (c-2min, c-5min and c-10min) and 2 wt% (d-2min) w/w SLNs. All data are means ± standard deviations for n = 3 replicates.

Day	Emulsion	d_{33}(μm)	σ	Free water (%)
0	a-2min	18.8 ± 1.2	0	0.200 ± 0.200
0	b-2min	19.0 ± 8.5	0	0
0	c-2min	18.4 ± 2.3	0.17 ± 0.04	0.054 ± 0.010
1	c-2min	21.3 ± 1.7	0.23 ± 0.01	0.041 ± 0.003
2	c-2min	24.3 ± 0.8	0.10 ± 0.00	0.230 ± 0.050
4	c-2min	40.0 ± 0.5	0.10 ± 0.00	0.300 ± 0.060
7	c-2min	15.0 ± 0.9	0	0.430 ± 0.020
0	c-5min	17.3 ± 0.2	0	0
0	c-10min	16.5 ± 1.6	0	0
0	d-2min	22.5 ± 1.3	0.24 ± 0.02	0.085 ± 0.009
1	d-2min	23.7 ± 1.7	0.24 ± 0.01	0.054 ± 0.003
2	d-2min	24.7 ± 0.2	0.26 ± 0.03	0.049 ± 0.002
4	d-2min	24.1 ± 1.9	0.22 ± 0.06	0.035 ± 0.004
7	d-2min	24.0 ± 0.3	0.29 ± 0.02	0.023 ± 0.002
10	d-2min	26.1 ± 0.6	0.33 ± 0.04	0.010 ± 0.001
14	d-2min	30.1 ± 0.2	0.29 ± 0.01	0.010 ± 0.001

The initial d_{33} value for emulsion c-2 was ~18 μm. By day 4, it increased to ~40 μm due to coalescence. The observed decrease at day 7 was likely the result of small-scale sedimentation that did not affect the macroscopic behaviour of the emulsion, but which resulted in seemingly erroneous droplet size readings (Fig. 6-3).

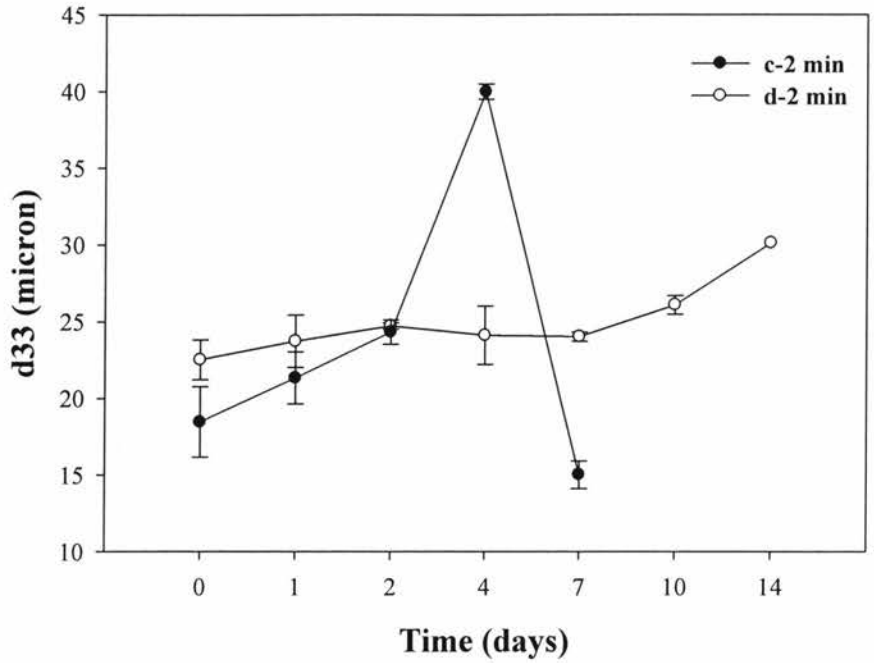

Figure 6-3: d_{33} evolution in emulsion c-2 min (containing 1.5% SLNs) and d-2 min (contains 2% SLNs). All data are means ± standard deviations for n=3 replication.

Fig. 6-3 also presents the d_{33} values for emulsions with 2% SLNs. As with the sedimentation data, this emulsion was also stable against coalescence for 14 days (Fig. 6-2 d-2 min). The NMR results (Fig. 6-3) showed that the d_{33} value increased from ~23 μm to ~ 30 μm over 14 days. By the end of day 7, there was no change in the average droplet diameter, with limited droplet growth seen at days 10 and 14.

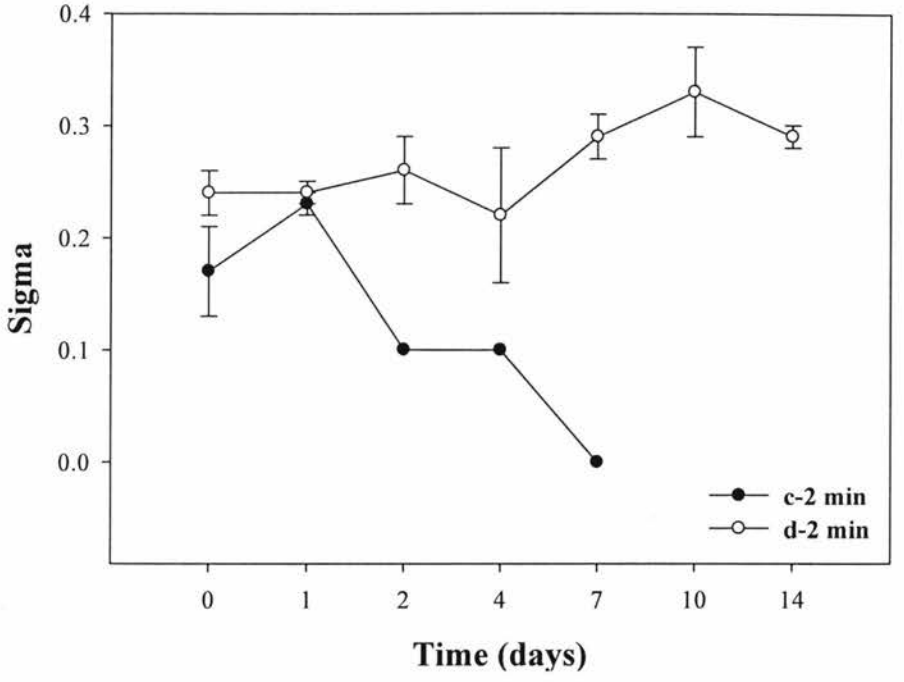

Figure 6-4: Evolution in σ in emulsions c-2 min and d-2 min. All data are means ± standard deviations for n=3 replicates.

In emulsion c-2 min, the σ value increased from ~0.17 to ~0.22 from day 0 to day 1, an indication of an increase in the breadth of the droplet size distribution as a result of coalescence (Fig. 6-4 and Fig. 6.6). There was also a decrease in the amount of free water from ~0.04 to ~0.01, though these results are inconclusive as the free water should have increased, given the emulsion's destabilisation (Fig. 6-5). Large increases in free water and σ were observed on subsequent days.

The evolution in droplet size distribution for emulsion c-2 min (Fig. 6-6) for day 0 to 4 showed a significant shift over 4 days. On day 0, the emulsion

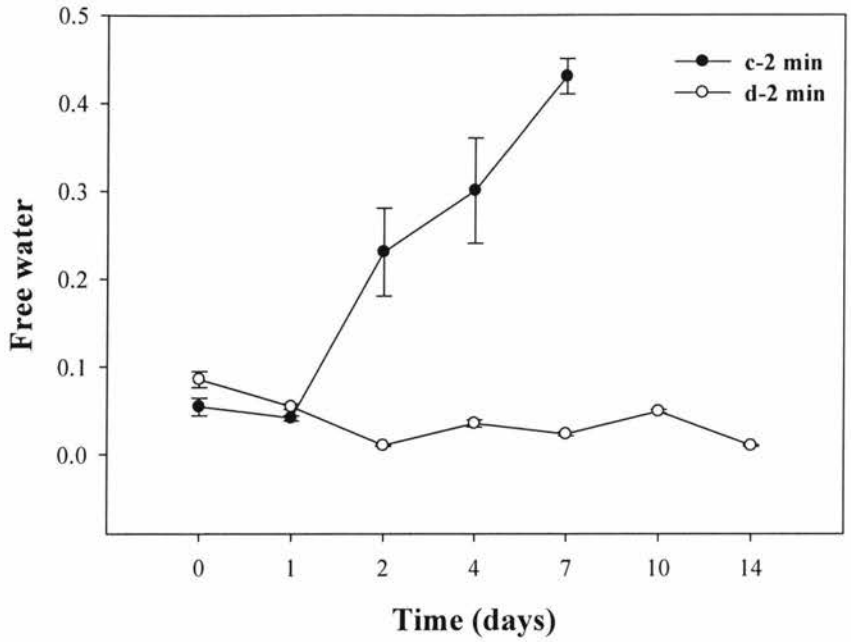

Figure 6-5: Free water evolution in emulsions c-2 min and d-2 min. All data are means ± standard deviations for n=3 replication.

distribution was narrow, but steadily increased so that by day 4, the mean droplet size was ~40 μm. However, there wasn't large increase in σ.

A narrow droplet size distribution was detected for the emulsion with 2% SLNs (d-2 min) (Fig. 6.7). The initial σ value was ~0.24 (day 0), which increased to ~0.3 by day 14, indicating that these emulsions gradually broadened in terms of droplet size distribution. There was little change in free water observed over the 14 days of study, a further indication that the emulsions were kinetically stable (Fig. 6-5).

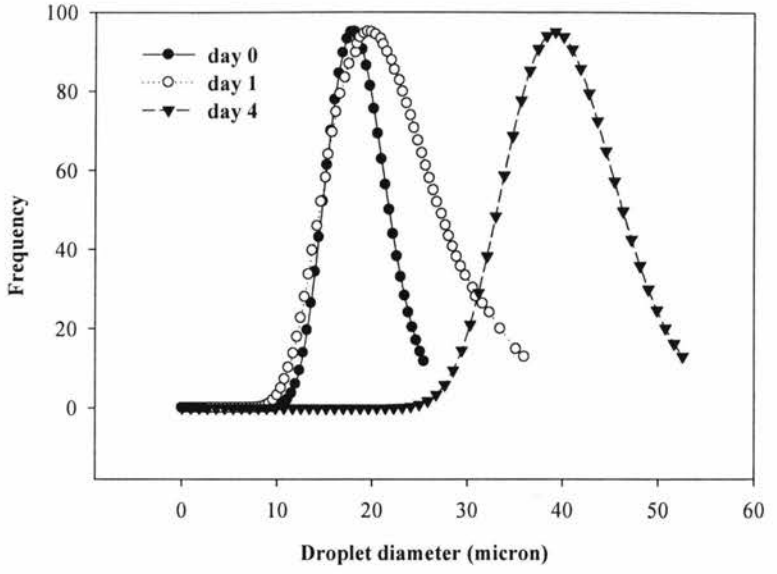

Figure 6-6: Evolution of log normal distribution for emulsion (c-2 min) from day 0 to 4.

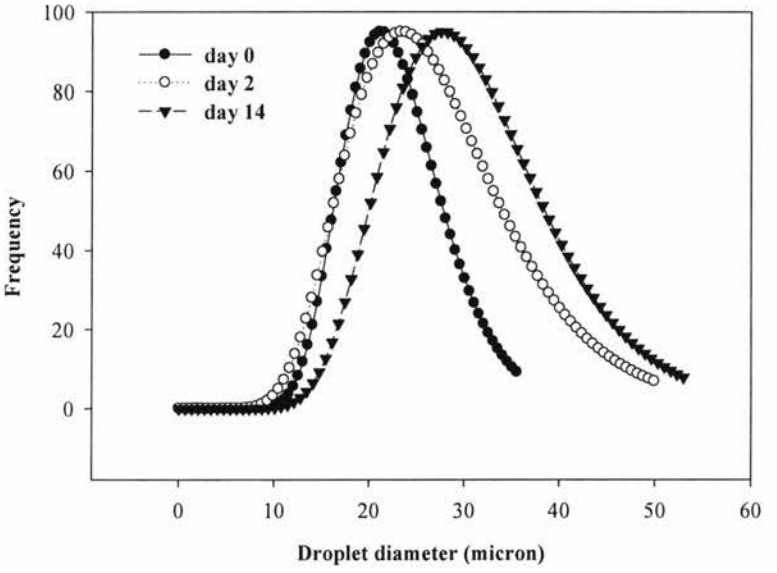

Figure 6-7: Evolution of log normal distribution for emulsion (d-2 min) from day 0 to 14.

6.3.4 Microscopy

Combined polarised light and confocal microscopy was used to examine the distribution of the monostearin SLNs in the emulsions and compare these observations with

sedimentation and NMR results. Images were captured on day 0 and when the emulsions destabilized, based on NMR results or on the last day of study (day 14) for emulsion d-2 min. The monostearin particle concentration necessary to stabilise these emulsions was determined as follows: based on NMR results, the mean water droplet diameter was ~ 25 μm, with the monostearin particles measuring ~ 650 nm, based on DLS. Both SLNs and water droplets were assumed spherical. The contact angle was considered 90°. Calculations for full monolayer coverage by spherical monostearin SLNs was calculated using surface area ($4 \pi r^2$) and volume ($4/3 \pi r^3$) determinations. The surface area of the water droplets was calculated as 1963.49 μm^2 (1.9634×10^{-9} m^2), which could be covered by 6041 monostearin particles with a surface area of 0.3318 μm^2 (0.3318×10^{-12} m^2) [SLN cross-section was assumed to be a flat circle with a surface area πr^2].

With the volume of one water droplet at 8181 μm^3 (8.181×10^{-15} m^3), the presence of 20% water in a 5 g emulsion (1 g or 1ml) yielded ~1.2×10^8 water droplets with a 25 μm diameter. If one droplet requires 6041 monostearin particles to be fully covered, there would be 7.2×10^{11} particles required to cover all droplets. If the volume of one monostearin particle is 0.1438 μm^3 (0.1438×10^{-18} m^3), 1.03×10^{11} μm^3 (1.03×10^{-7} m^3), would be needed, which is ~ 7.7-8.2 mg (monostearin specific gravity = 0.75-0.80 g/ml). Based on these calculations, ~1.5-2% SLNs in a 5 g emulsion should be sufficient for a dense, monolayer coverage. NMR results showed that stability was best achieved with 2% SLNs.

Fig. 6-8 shows the microstructure of emulsion a-2 min at day 0. The fluorescence images (Fig. 6-8A) showed droplets surrounded by monostearin crystals (highlighted in Fig. 6-8B) located around the droplets and within the oil phase. The interface between coalescing droplets was covered by SLN crystals (Fig. 6-8C).

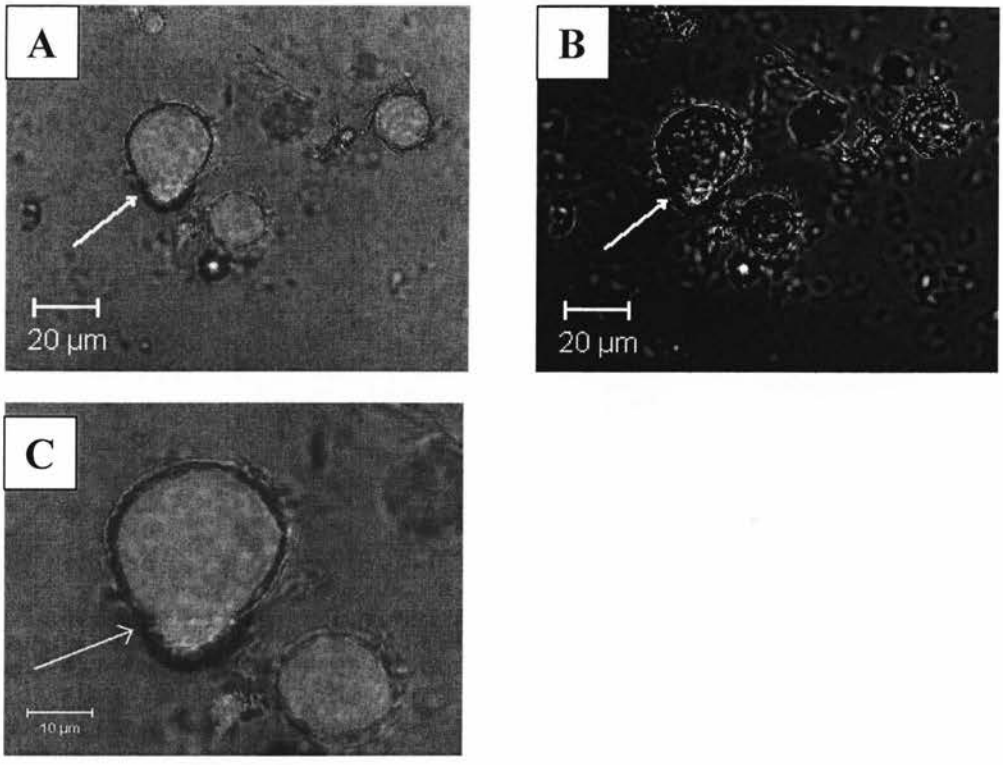

Figure 6-8: Emulsion a-2 min at day 0. (A) is the fluorescence image of the emulsion; (B) is the matching polarised light view; (C) shows enlarged droplets.

An SLN content of 1 wt % did not improve emulsion stability (Fig. 6-9) as emulsion b-2 min was not stable due to lack of monostearin crystals.

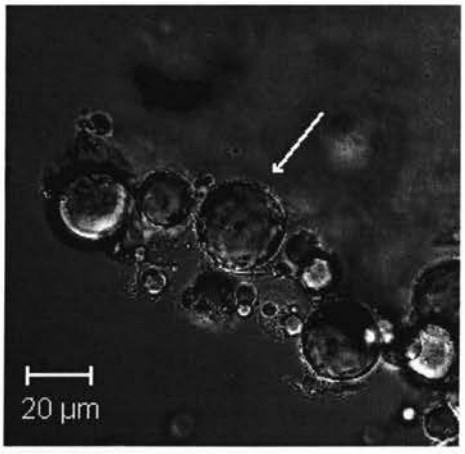

Figure 6-9: Polarised light image of emulsion b-2 min at day 0.

With 1.5 wt % added monostearin (Fig. 6-10A and B), droplets were ~ 20-30 μm in diameter and were covered by a thin layer of particles. Most SLNs were at the interface, though some resided in the oil phase (arrows in 6.10B).

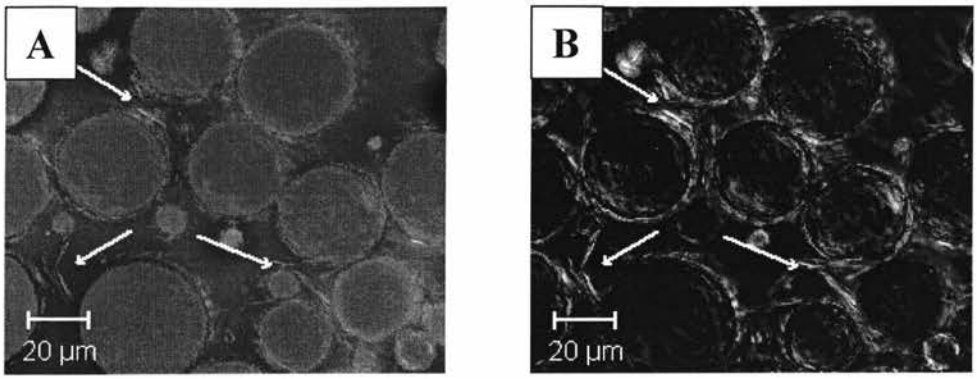

Figure 6-10: CLSM images (combined and polarised) for emulsion c-2 min (day 0). Image A is the combined fluorescence and polarised image of the water and oil phases and image B is the polarised light image.

Based on NMR, emulsion c-2 min started to destabilise at day 4. Images taken on the same day (Fig. 6-11) confirmed that there was coalescence (Fig. 6-11A). The droplet in the square showed multilayer coverage with monostearin crystals as well as continuous phase crystals between the droplets, suggesting that Pickering and crystal network stabilisation were both prevalent.

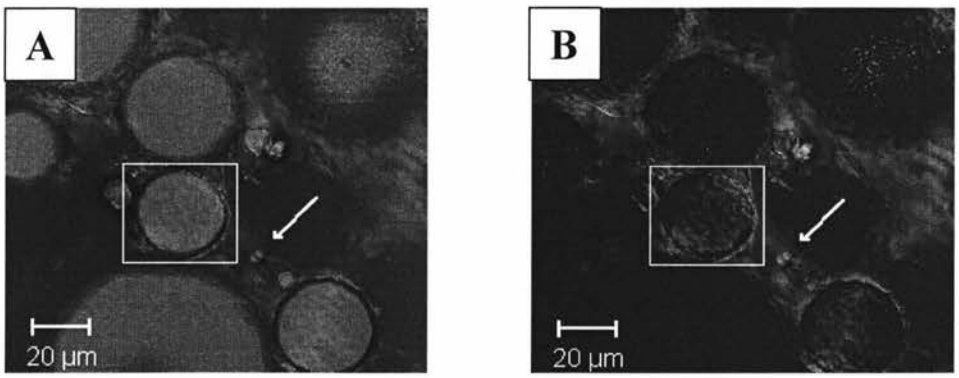

Figure 6-11: Emulsion c-2 min on day 4. (A) is the fluorescence image of the emulsion; (B) is the matching polarised light view.

Emulsions c-5 min and c-10 min (Figs 6-12 and 6-13) had droplet size distributions similar to emulsion c-2 min. However, they coalesced quickly (NMR results), which was likely due to heat-induced SLN accretion, which resulted in larger SLNs incapable of effectively stabilising the dispersed droplets via a Pickering mechanism [103].

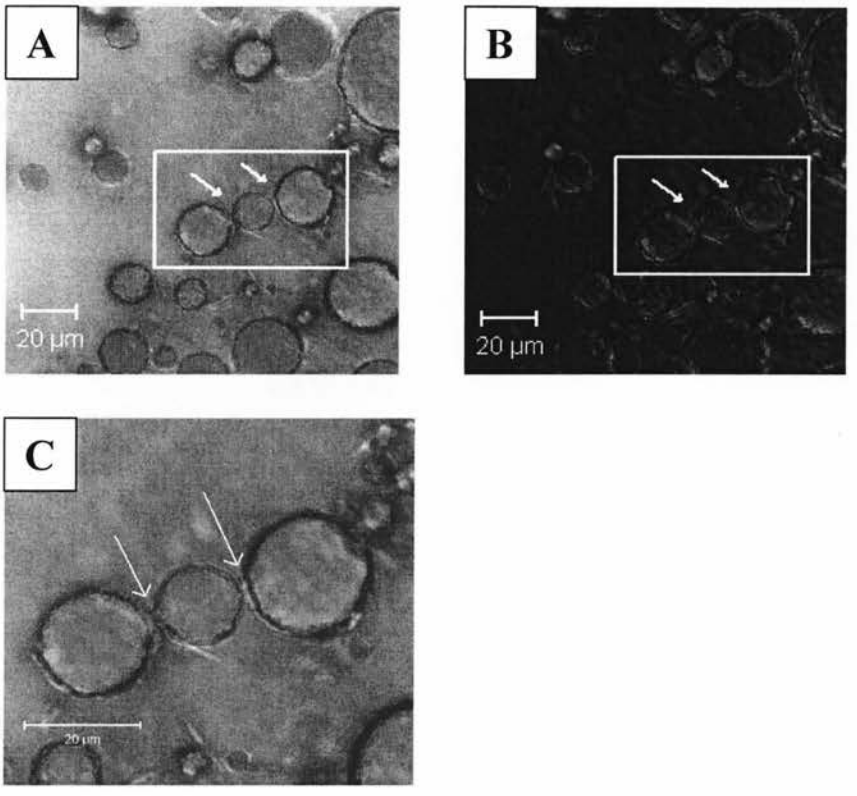

Figure 6-12: Emulsion c-5 min at day 0. (A) is the fluorescence image of the emulsion; (B) is the matching polarised light view; Arrows in (C) shows evidence of Pickering stabilisation.

When the emulsion was homogenised for 10 minutes (Fig. 6-13), water droplets 10-30 µm in diameter were observed, in agreement with NMR results, which yielded a d_{33} of 17 µm (Fig. 6-13A and B). Most droplets were covered by monolayer or multilayer monostearin, indicative of extensive Pickering stabilisation. The lack of stability (*e.g.*, see sedimentation results) may perhaps be attributed to the formation of larger crystals during homogenisation through crystal-crystal accretion. Such large crystals would be unable to effectively form a

monolayer around the droplets. An unusual feature warranting further attention is the droplet deformation caused by the monostearin (Fig. 6-13C and D). At this juncture, this phenomenon remains unexplained.

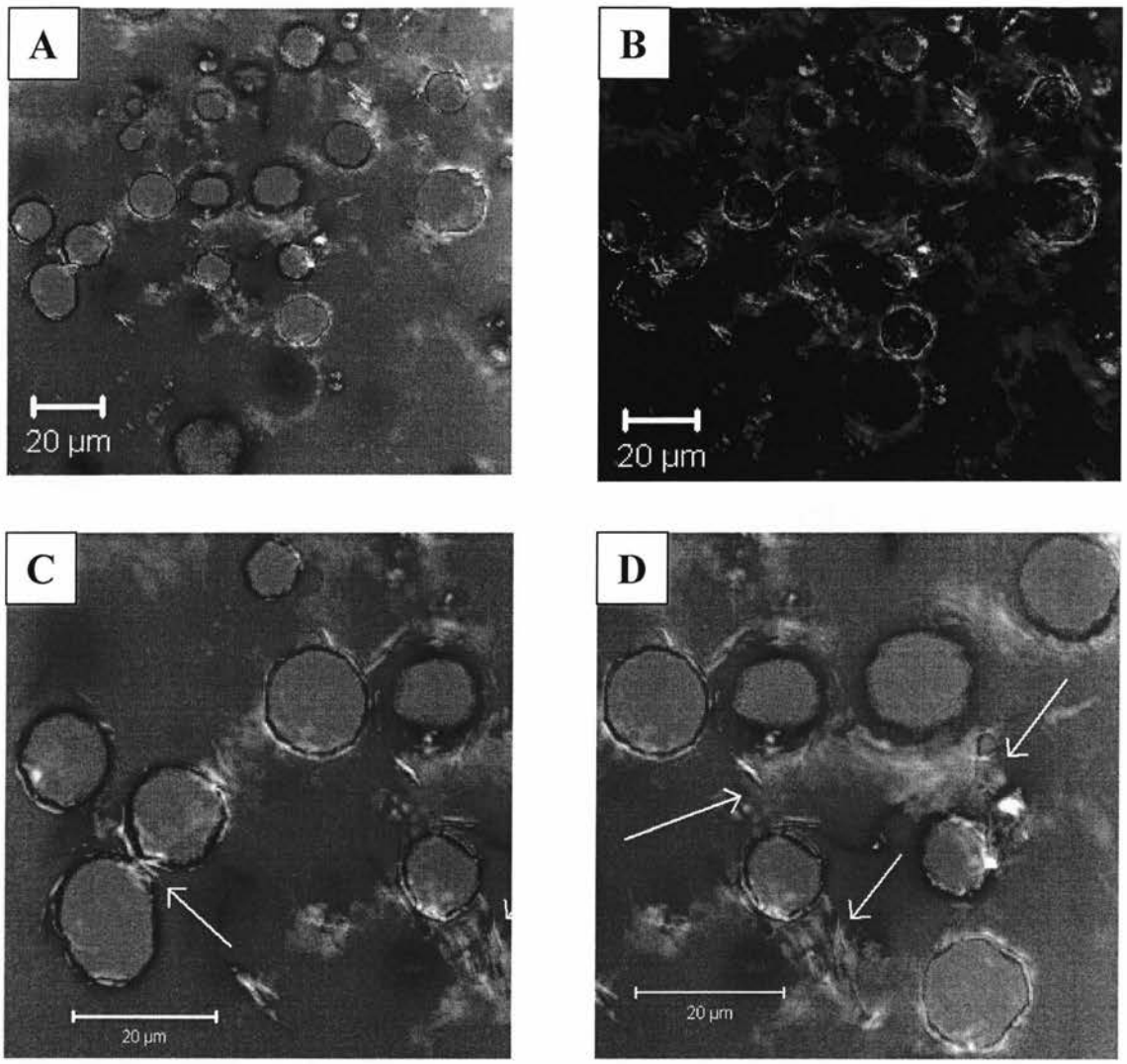

Figure 6-13: Emulsion c-10 min at day 0. (A) is the fluorescence image of the emulsion; (B) is the matching polarised light view; (C) shows the Pickering effect; and (D) shows the SLN crystal network.

Emulsion d-2 min (Fig. 6.14) was stable during the entire study. It remained macroscopically monophasic and showed little change in droplet size. In Fig 6-14A and B, water droplets ~20-25 µm in diameter (which is in an agreement with NMR results) were

covered by thick (~3-5 μm) monostearin multilayer films not observed in other emulsions (see arrows in Fig. 6.14C).

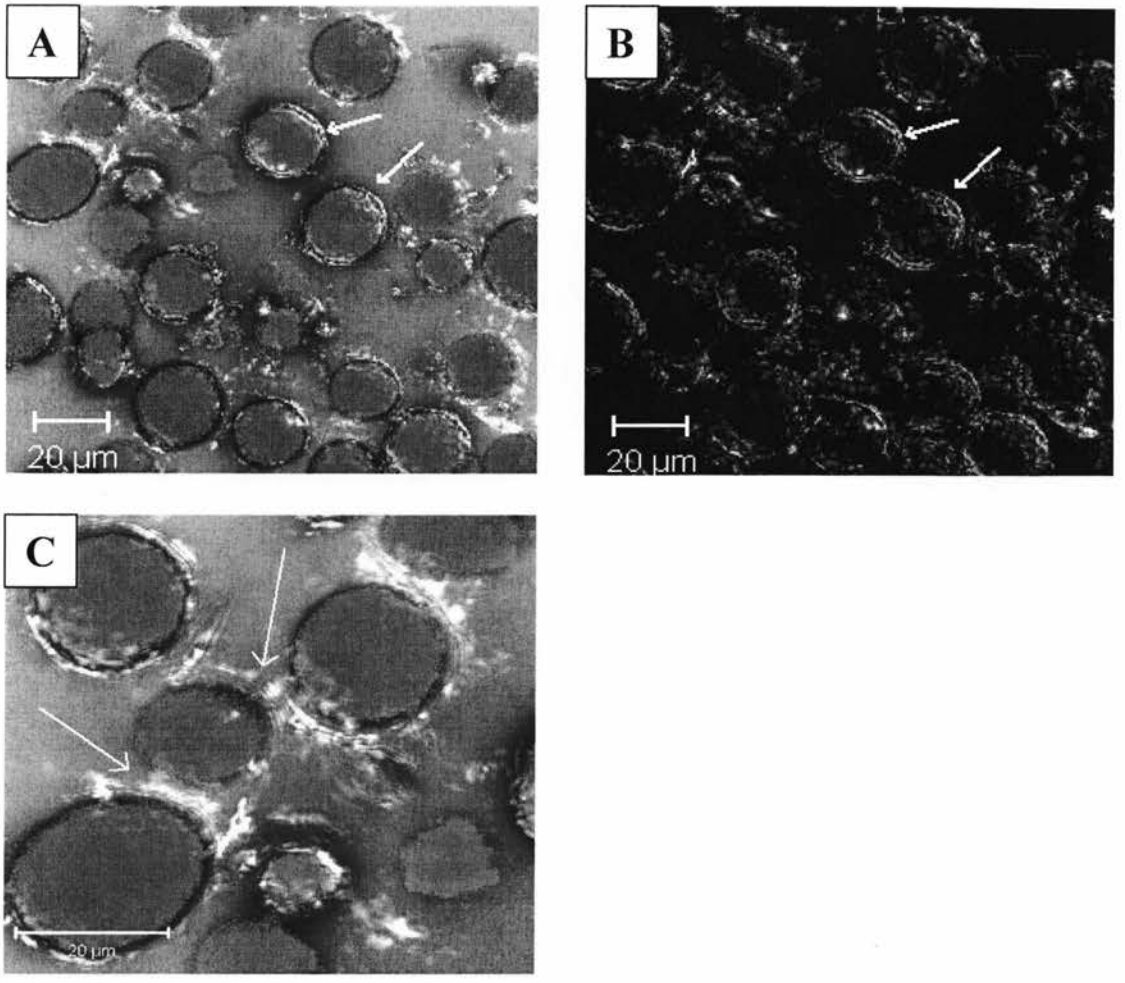

Figure 6-14: Emulsion d-2 min at day 0. (A) is the fluorescence image of the emulsion; (B) is the matching polarised light view; Arrows in (C) shows evidence of Pickering stabilisation.

At day 14 (Fig. 6-15), there was a slight increase in droplet size (Fig. 6.15A) compared to day 0. Furthermore, the arrows in Fig. 6.15B showed small crystals adsorbed to the oil-water interface. Monostearin particles too large to be adsorbed at the interface were seen in the continuous oil phase either as aggregates or individual needles. These results demonstrated

that surface-active monostearin particles could be located either at interface or in the oil phase based on their size.

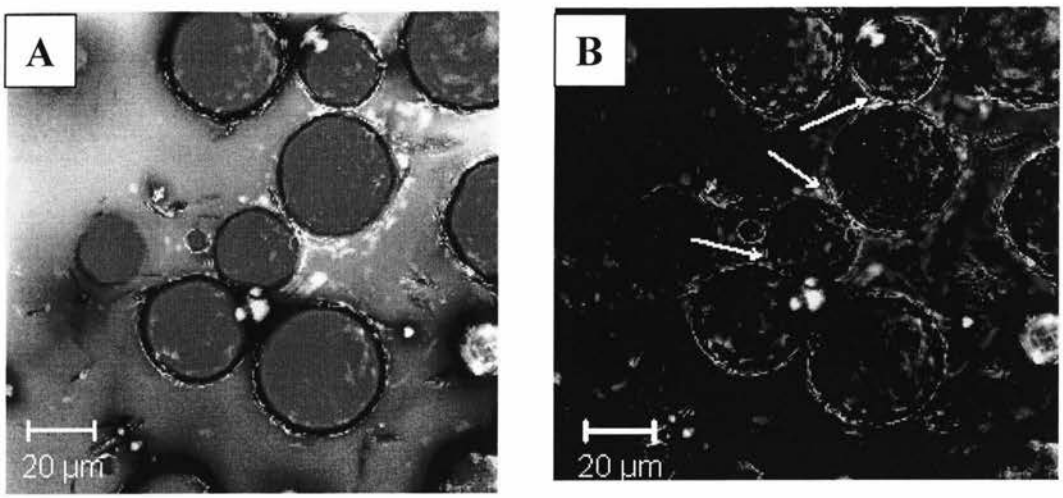

Figure 6-15: Emulsion d-2 min at day 14. (A) is the fluorescence image of the emulsion; (B) is the matching polarised light view.

6.4 Conclusions

The initial particle size of the SLNs increased from ~120 nm to ~ 650 nm after centrifugation. These particles were used to stabilise 20% (w/w) W/O emulsions. Based on surface energetics, the particles were located at the oil-water interface with an equilibrium contact angle of ~ 115°, indicative of W/O emulsion stabilisation.

Different SLN concentrations [0.5, 1, 1.5, and 2% (w/w)] were used to make emulsions and the resulting emulsions were evaluated for sedimentation, droplet size distribution and microstructure. Emulsions with 2% (w/w) SLNs were most resistant to breakdown. Using microscopy, multilayered monostearin particles were visible around the dispersed aqueous droplets, which was evidence of Pickering stabilisation. There was also an indication of network stabilisation, given the existence of aggregated monostearin crystals in the oil phase. It

thus appears that both Pickering stabilisation and the presence of an SLN crystal network slowed droplet-droplet coalescence.

Chapter 7

Overall conclusions

Stable W/O emulsions were prepared by using monostearin nanoparticles which were produced via a microemulsion method. O/W microemulsions consisting of monostearin, Tween 20, ethanol, and water were formulated and characterised. For effective microemulsion formation, the types of surfactant and co-surfactant were key to achieving stability, with the combination of Tween 20 and ethanol at 1.5:1 ratio deemed most effective for generation of monostearin-based O/W microemulsions. The phase behaviour of a selected dilution line permitted the characterisation of a portion of the monophasic O/W region. The microemulsion with the highest content of monostearin was chosen as a nano-reactor for SLN development.

A crystallisation study was performed to establish the super-cooling method in which liquid monostearin (present in the hot microemulsion) solidified. The size of the SLNs was small (~120 nm), as detected by DLS and confirmed by AFM imaging. DSC was used to confirm the liquid-solid transition of the monostearin. Lecithin was used to stabilise the SLN suspension by increasing the ζ-potential to - 40, though this did not entirely prevent aggregation. Centrifugation was used to remove excess water from the SLN suspension. This method increased particle-particle collisions, thereby increasing SLN particle size from 120 nm to ~ 650 nm. These particles were used to stabilise a model W/O emulsion.

An equilibrium contact angle ($\theta \sim 115^{\circ}$) indicated that the monostearin particles would stabilise aqueous droplets in an oil-continuous environment, with the detachment energy indicating firm particle attachment to the interface.

The separated nanoparticles were used at 0.5, 1, 1.5 and 2 wt % to stabilise 20% water in mineral oil emulsions. Sedimentation and pfg-NMR measurements showed that the diameter of the aqueous phase within the emulsion with 2 wt % SLNs increased by ~8 μm over 14 days. Overall, microscopy images were in a good agreement with pfg-NMR results. The presence of interfacial monostearin SLNs was confirmed by polarised light microscopy, where both Pickering and network crystals appeared to play a role in stabilisation. Overall, this study demonstrated that it is possible to kinetically stabilise W/O emulsions using solid lipid nanoparticles.

Chapter 8

Future studies

Areas for further studies include:

1. Improvement of SLN stability. In this study, a microemulsion system was used as a nano-reactor to develop SLNs. However, this approach led to complications regarding the stability of the harvested SLNs. In this light, other methods for SLN development such as hot valve homogenisation should be attempted. Though each method has its drawbacks, hot homogenisation would also allow for more rapid 'mass' production of these SLNs.

2. The method for harvesting SLNs should be improved. The method used in this study was based on centrifugation, which led to SLN aggregation and an increase in particle size. Filtration was examined as another solution to this problem, but this method was slow and there was SLN adhesion to the surface of the filter. In future, freeze-drying could be attempted, though there are drawbacks, as mentioned in the literature [97].

3. Homogenisation was performed with a small-volume impeller-type homogeniser. The main issue with this technique is emulsion temperature control, as high temperatures may have melted the SLNs. Temperature was controlled by placing the homogenisation chamber in a cold bath, though for future studies, better temperature control should be attempted.

4. The presence of monostearin crystals in the continuous oil phase of the W/O emulsion may have resulted from the centrifugation and homogenisation steps, which may have led to the formation of larger crystals. By optimising the harvesting method and

subsequent homogenisation, the concentration of SLNs required to stabilise the emulsions could be fine-tuned so that monostearin particles are only present at interfaces and not in the oil phase.

5. Fundamental studies of the monostearin particles' behaviour at the interface should be attempted. For example, what happens to the particles when they first migrate to the interface? Do they change in size via aggregation? Similarly, would there be a way of controlling interfacially-adsorbed colloid particle size? This may serve as a means to better tailor the stabilisation effect of the SLNs.

References:

1. Leal-Calderon, F., Bibette, J., Schmitt, V., Emulsion Science: Basic Principles, Springer, NY, 2007, chapter 1, pp. 1- 4.

2. McClements, D.J., Food Emulsions: Principles, Practices and Technology, 2nd edition, edited by: Raton, B., 2005, chapter 1, pp. 1-27,.

3. McClements, D.J., Food Lipids: Chemistry, Nutrition, and Biotechnology, 2nd edition, edited by: Akoh, C.C., Min, D.B., 1998, chapter 3, pp. 63- 103.

4. Eskanda, N.G., Simovic, S., Prestidge, C.A., Synergistic effect of silica nanoparticles and charged surfactants in the formation and stability of submicron oil-in-water emulsions, Physical Chemistry and Chemical Physics, 9, 2007, 6426-6434.

5. Melle, S., Lask, M., Fuller, G.G., Pickering emulsions with controllable stability, Langmuir, 21, 2005, 2158-2162.

6. Binks, B.P., Lumsdon, S.O., Stability of oil-in-water emulsions stabilized by silica particles, Physical Chemistry and Chemical Physics, 1, 1999, 3007-3016.

7. Binks, B.P., Lumsdon, S.O., Pickering emulsions stabilized by monodisperse latex particles: effect of particle size, Langmuir, 17, 2001, 4540-4547.

8. Ashby, N. P., Binks, B.P., Pickering emulsions stabilised by laponite clay particles, Physical Chemistry and Chemical Physics, 2, 2000, 5640-5646.

9. Aveyard, R., Binks, B. P., Clint, J.H., Emulsions stabilised solely by colloidal particles, Advances in Colloid and Interface Science, 2003, 503-546.

10. Rousseau, D., Fat crystal behaviour in food emulsions, Physical Properties of Lipids, edited by: Marangoni, A. G., 2002, chapter 8, pp. 219-264.

11. Hodge, S. M., Rousseau, D., Continuous-phase fat crystals strongly influence water-in-oil emulsion stability, Journal of the American Oil Chemists' Society, 3, 2005, 159-164.

12. Levine, S., Bowen, B. D., and Patridge, S. J., Stabilisation of emulsions by fine particles I. Partitioning of particles between continuous phase and oil-water interface, Colloids and Surfaces, 38, 1989, 325-343.

13. Johansson, D., Bergenstahl, B, The influence of food emulsifiers on fat and sugar dispersion in oils. II. Rheology, colloidal forces. Journal of the American Oil Chemists' Society 69, 1992, 718-727.

14. Tambe, D. E., Sharma, M. M., The effect of colloidal particles on fluid-fluid interfacial properties and emulsion stability, Advances in Colloid and Interface Science, 52, 1994, 1-63.

15. Rousseau, D., Fat crystals and emulsion stability- A review. Food Research International, 33, 2000, 3-14.

16. Johansson, D., Bergenstahl, B., Lundgren E., Water-in-triglyceride oil emulsions: effect of fat crystals on stability. Journal of the American Oil Chemists' Society, 72, 1995, 939-950.

17. Midmore, B. R., Preparation of a novel silica-stabilised oil/water emulsion, Colloids and Surfaces A : Physicochemical and Engineering Aspects, 132 , 1998, 257-265.

18. Garti, N., aserin, A., Tiunova, I., Benyamin, H., Double emulsions of W/O/W stabilised by fat microcrystals. Part I. Selection of emulsifiers and fat microcrystalline particles, Journal of the American Oil Chemists' Society 76, 1999, 383-389.

19. Churaev, N. V., The DLVO theory in Russian colloid science, Advances in Colloid and Interface Science, 83, 1999, 19-32.

20. Fornes, J. A., Secondary minimum analysis in the DLVO theory, Colloid & Polymer Science, 263, 1985, 1004-1007.

21. Verwey, E.J.W., Overbeek, J.Th.G., Theory of the Stability of Lyophobic Colloids, Elsevier, Amsterdam, 1948.

22. Chang, Y. I., Ku, M. H., Gravity-induced flocculation of non-Brownian particles, Colloids and surfaces A: Physicochemical and Engineering Aspects, 178, 2001, 231-247.

23. McClements, D. J., Food Lipids Chemistry, Nutrition, and Biotechnology,2nd edition, edited by: Akoh, C.C., Min, D.B., 1998, chapter 3, pp. 89-95.

24. McClements, D.J., Food emulsions Principles, practices, and technology, 2nd edition, edited by: Raton, B., CRC press, 2005, chapter 7, P. 269-339.

25. Ratke, L., Voorhees, P. W., Growth and coarsening: Ostwald Ripening in material processing. Springer, 2002, 117-118. Retrieved on 2007-11-15.

26. Anton, N., Benoit, J. P., Saulnier, P., Design and production of nanoparticles formulated from nano-emulsion template-A review, Journal of Controlled Release, 2008, article in press.

27. Binks, B. P., Particles as surfactants-Similarities and differences, Current Opinion in Colloid & Interface Science 7, 2002, 21-41.

28. Lopentinsky, R. J. G., Masliyah, J. H., Xu, Z., Solids-stabilised emulsions: A review, Colloidal particles at liquid interfaces, edited by: Binks, B. P., Horozov, T. S., 2005, chapter 6, 186-224.

29. Thieme, J., Abend, S., Lagaly, G., Aggregation in Pickering emulsions, Colloid & Polymer Science, 277, 1999, 257-260.

30. Abend, S., Bonnke, N., Gutschner, U., Lagaly, G., Stabilisation of emulsions by heterocoagulation of clay minerals and layered double hydroxide, Colloid & Polymer Science, 276, 1998, 730-737.

31. Binks, P. B., Whitby, C. P., Silica particle-stabilised emulsions of silicone oil and water: aspects of emulsification, Langmuir, 20, 2004,1130-1137.

32. Binks, P. B., Lumsdon S. O., Pickering emulsions stabilised by monodispersed latex particles: Effects of particle size, Langmuir, 17, 2001, 4540-4547.

33. Binks, P. B., Lumsdon S. O., Influence of particle wettability on the type and stability of surfactant-free emulsions, Langmuir, 16, 2000, 8622-8631.

34. Johansson, D., Bergenstahl, B., Lecithins in oil-continuous emulsions – Fat crystal wetting and interfacial tension, Journal of the American Oil Chemist's Society, 72, 1995, 205-211.

35. Lin, Y., Boker, A., Skaff, H., Cookson, D., Dinsmore, A. D., Emrick, T., Russell, T. P., Nanoparticle assembly at fluid interfaces: structure and dynamics, Langmuir, 21, 2005,191-194.

36. Dai, L. L., Sharma, R., Wu, C. Y., Self-assembled structure of nanoparticles at a liquid-liquid interface, Langmuir, 21, 2005, 2641-2643.

37. Cauvin, S., Colver, P. J., Bon, S. A. F., Pickering stabilised miniemulsion polymerisation: preparation of clay armoured latexes, Macromolecules, 38, 2005, 7887-7889.

38. Vignati, E., Piazza, R., Lockhart, T.P., Pickering emulsions: Interfacial tension, colloidal layer morphology and trapped particle motion, Langmuir, 19, 2003, 6650-6656.

39. Dickinson, E., Interfacial particles in food emulsions and foams in Colloidal particles in liquid interfaces, edited by: Binks, B. P., Horozov, T. S., 2005, chapter 8, 298-327.

40. Fleer, G.J., Cohen Stuart, M.A., Scheutjens, J.M.H.M., Cosgrove, T., Vincent, B., Polymers at interfaces, Chapman and Hall, London, 1993.

41. Johansson, B., Lindman, B., Holmberg, K., Kronberg B., Surfactants and polymers in aqueous solution. John Wiley & Sons, Chichester, UK, 1998.

42. Binks, B.P., Lumsdon S.O., Stability of oil-in-water emulsions stabilised by silica particles. Physical Chemistry & Chemical Physics, 1999, 1, 3007-3016.

43. Wissing S. A., Kayse O., Muller R.H., Solid lipid nanoparticles for parenteral drug delivery, Advanced Drug Delivery Reviews, 56, 2004,1257-1272.

44. Heurtault, B., Saulnier, P., Pech, B., Proust, J.E., Benoit, J. P., Physico-chemical stability of colloidal lipid particles, Biomaterials, 24, 2003, 4283-4300.

45. Gasco, M. R., Method for producing solid lipid microspheres having a narrow size distribution, US. Patent No. 5250236, 1993.

46. Cavalli, R., Marengo, E., Rodriguez, L., Gasco, M. R., Effects of some experimental factors on the production process of solid lipid nanoparticles, European Journal of Pharmaceutics and Biopharmaceutics, 43, 1996,110– 115.

47. Gasco, M. R., solid lipid nanospheres from warm microemulsions, Pharmaceutical Technology Europe, 9,1997, 52-58.

48. Cortesi, R., Esposito, E., Luca, G., Nastruzzi, C., Production of lipospheres as carriers for bioactive compounds, Biomaterials, 23, 2002, 2283– 2294.

49. Cavalli, R., Caputo, O., Marengo, E., Pattarino, F., Gasco, M. R., The effect of the components of microemulsions on both size and crystalline structure of solid lipid nanoparticles (SLN) containing a series of model molecules, Pharmazie, 53, 1998, 392– 396.

50. Igartua, M., Saulnier, P., Heurtault, B. Pech, B., Proust, J. E., Pedraz, J. L., Benoit, J.P., Development and characterization of solid lipid nanoparticles loaded with magnetite, International Journal of Pharmaceutics, 233, 2002, 149–157.

51. Muller, R.H., Mader, K., Gohla, S., Solid lipid nanoparticles (SLN) for controlled drug delivery- a review of the state of the art, European Journal of Pharmaceutics and Biopharmaceutics, 50, 2000, 161-177.

52. Marengo, E., Cavalli, R., Capto, O., Rodriguez, L., Gasco, M., Scale-up of the preparation process of solid lipid nanospheres. Part I, International Journal of Pharmaceutics, 205, 2000, 3-13.

53. Moulik, S.P., Paul, B.K., Structure, dynamics and transport properties of microemulsions, Advances in Colloid and Interface Science, 78, 1998, 99-195.

54. Polizelli, M. A., Telis, V. R. N., Amaral, L., Feitosa, E., Formation and characterization of soy bean oil/surfactant/water microemulsions, Colloids and Surfaces A: Physicochemical and Engineering Aspects, 281, 2006, 230-236.

55. Campo, L., Yaghmur, A., Garti, N., Leser, M., E., Folmer, B., Glatter, O., Five-component food-grade microemulsions: structural characterization by SANS, Journal of Colloid and Interface Science, 274, 2004, 251-267.

56. Ronzer, S., Aserin, A., Wachtel, E., J., Garti, N., Competitive solubilisation of cholesterol and phytosterols in nonionic microemulsions, Journal of Colloid and Interface Science, 314, 2007, 718-726.

57. Garti, N., Aserin, A., Ezraih, S., Wachtel, E., Water solubilisation and chain length compatibility in nonionic microemulsions, Journal of Colloid and Interface Science, 169, 1995, 428-436.

58. Yaghmur, A., Aserin, A., Garti, N., phase behaviour of microemulsions based on food-grade nonionic surfactants: effect of polyols and short-chain alcohols, Colloids and Surfaces A: Physicochemical and Engineering Aspects, 209, 2002, 71-81.

59. Garti, N., Spernath, A., Aserin, A., Lutz, R., Nano-sized self-assemblies of nonionic surfactants as solubilisation reservoirs and microreactors for food systems, Soft Matter, 1, 2005, 206-218.

60. Aboofazeli, R., Lawrence, C. B., Wicks, S. R., Lawrence, M. J., Investigations into the formation and characterization of phospholipids microemulsions. III. Pseudo-ternary phase diagrams of systems containing water-lecithin-isopropyl myristate and either an alkanoic acid, amine, alkanediol, polyethylene glycol alkyl ether or alcohol as co-surfactant, International Journal of Pharmaceutics, 111, 1994, 63-72.

61. Shinoda, K., Lindman, B., Organised surfactant systems: microemulsions, Langmuir, 3, 1987, 135-149.

62. Caboi, F., Lazzari, P., Pani, L., Monduzzi, M., Effect of 1-butanol on the microstructure of lecithin/water/tripalmitin system, Chemistry and Physics of Lipids, 135, 2005, 147-156.

63. Gupta, S., Moulik, S.P., Lala, S., Basu, M.K., Sanyal, S.K., Datta, S., Designing and testing of an effective oil-in-water microemulsion drug delivery system for in vivo application, Drug Delivery, 12, 2005, 267-273.

64. Winsor, P. A., Hydrotropy, solubilisation, and related emulsification processes, Transactions of the Faraday Society, 44, 1948, 376-398.

65. Shukla, A., Janich, M., Jahn, K., Neubert, R.H. H., Microemulsions for dermal drug delivery studied by dynamic light scattering: Effect of interparticle interactions in oil-in-water microemulsions., Journal of Pharmaceutical Sciences, 92, 2003, 730-738.

66. Fanun, M., Surfactant chain length effect on the structural parameters of nonionic microemulsions, Journal of Dispersion Science and Technology, 29, 2008, 289-296.

67. Garti, N., Food emulsifiers, Physical properties of lipids, edited by: Marangoni, A. G., chapter 9, 265-386.

68. Matsuzawa, H., Murakami, K., Iwahashi, M., Comparison of hydrogen bonding for chiral and racemic 1-monostearoylglycerols in solvent, Journal of Oleo Science, 57, 2008, 287-292.

69. Hu, F.Q., Yuan, H., Zhang, H.H., Fang, M, Preparation of solid lipid nanoparticles with clobetasol propionate by a novel solvent diffusion method in aqueous system and physicochemical characterization, International Journal of Pharmaceutics, 239, 2002, 121-128.

70. Yuan, H., Miao, J., Du, Y. Z., You, Y., Hu, F.Q., Zeng, S., Cellular uptake of solid lipid nanoparticles and cytotoxicity of encapsulated paclitaxel in A549 cancer cells, International Journal of Pharmaceutics,348, 2008,137-145.

71. McClements, D.J., Food emulsions Principles, practices, and technology, 2nd edition, edited by: Raton, B., CRC press, 2005, chapter 4, 95-175.

72. Nagarajan R., Ruckenstein E., Aggregation of amphiphiles as micelles or vesicles in aqueous media, Journal of Colloid and Interface Science, 71, 1979, 580-604.

73. Christian S.D., Scamehorn, J.F., Solubilisation in surfactant aggregates, edited by: Dekker, M., New York, NY., 1995, 3-35.

74. Zhang, H.H., Feng F.Q., Li, J., Zhan, X., Wei, H.W., Li, H., X., Wang H.Y., Zheng X.D., Formulation of food-grade microemulsions with glycerol monolaurate: effects of short chain alcohols, polyols, salts, and nonionic surfactants., European Food Research and Technology,226, 2008, 613-619.

75. Shome, A., Roy, S., Das P.K., Nonionic surfactants: a key to enhance the enzyme activity at cationic reverse micellar interface., Langmuir, 23, 2007, 4130-4136.

76. Rao, I.V., Ruckenstein E., Micellisation behaviour in the presence of alcohols, Journal of Colloid and Interface Science,113, 1986, 375-387.

77. Fanun, M., Phase behaviour, transport, diffusion and structural parameters of nonionic surfactants microemulsions, Journal of Molecular Liquids, 139, 2008, 14-22.

78. El Maghraby, G.M., Transdermal delivery of hydrocortisone from eucalyptus oil microemulsion: effects of co-surfactants, International Journal of Pharmaceutics, 355, 2008, 285-292.

79. You, J., Wan, F., de Cui, F., Sun, Y., Du, Y.Z., Hu, F.Q., Preparation and characterization of vinorelbine bitartrate-loaded solid lipid nanoparticles, International Journal of Pharmaceutics, 343, 2007, 270-276.

80. Battaglia, L., Trotta, M., Gallarate, M., Carlotti, M. E., Zara, G., P., Bargoni, A., Solid lipid nanoparticles formed by solvent-in-water emulsion diffusion technique: development and influence on insulin stability, Journal of Microencapsulation, 24, 2007, 672-684.

81. Fellers, T. J., Davidson, M.W., Introduction to Confocal Microscopy. Olympus Fluoview Resource Center. National High Magnetic Field Laboratory, 2007, Retrieved on 2008-07-10.

82. Tanner, I.E., Stejskal, E. O., Restricted Self-diffusion of Protons in Colloidal Systems by the Pulsed-Gradient, Spin-Echo Method, Journal of Chemical Physics, 49, 1968,1768-1777.

83. Fourel, L, Guillement, J. P., Le Botlan, D., Determination of Water Droplet Size Distributions by Low Resolution PFG-NMR: I. "Liquid" Emulsions, Journal of Colloid and Interface Science, 764, 1994, 48-53.

84. Fourel, L, Guillement, J. P., Le Botlan, D., Determination of Water Droplet Size Distributions by Low Resolution PFG-NMR: II. "Solid" Emulsions, Journal of Colloid and Interface Science, 769, 1995, 119-125.

85. Muhlen, A., Muhlen, E., Niehus, H., Mehnert, W., Atomic force microscopy studies of solid lipid nanoparticles, Pharmaceutical Research, 13, 1996, 1411-1416.

86. Leung, R., Shah, D., O., Solubilisation and phase equilibria of water-in-oil microemulsions I. effects of spontaneous curvature and elasticity of interfacial films, Journal of Colloid and Interface Science, 120, 1987, 320-328.

87. Leung, R., Shah, D., O., Solubilisation and phase equilibria of water-in-oil microemulsions II. Effects of alcohols, oils, and salinity on single chain surfactant systems, Journal of Colloid and Interface Science, 120, 1987, 330-344.

88. Fanun, M., Conductivity, viscosity, NMR and diclofenac solubilisation capacity studies of mixed nonionic surfactants microemulsions, Journal of Molecular Liquids, 135, 2007, 5-13.

89. Kogan, A., Popov, I., Uvarov, V., Cohen, S., Aserin, A., Garti, N., Crystallization of carbamazepine pseudopolymorphs from nonionic microemulsions, Langmuir,24, 2008, 722-733.

90. Schulz, P. C., Soltero, J. F. A., Puig, J. E., DSC analysis of surfactant-based microstructures, in Thermal Behaviour of Dispersed Systems, edited by: Nissim Garti, 2000, chapter 4, 121-181.

91. Bunjes, H., Koch, M. H. J., Westesen, K., Effect of particle size on colloidal solid triglycerides., Langmuir, 16, 2000, 5234-5241.

92. Bunjes, H., Steiniger, F., Richter, W., Visualising the structure of triglyceride nanoparticles in different crystal modifications, Langmuir, 23, 2007, 4005-4011.

93. Siekmann, B., Westesen, K., Thermoanalysis of the recrystallisation process of melt-homogenised glyceride nanoparticles, Colloids and Surfaces B. Biointerfaces, 3, 1994, 159-175.

94. Unruh, T., Bunjes, H., Westesen, K., Koch, M.H.J., Investigations on the melting behaviour of triglyceride nanoparticles, Colloid & Polymer Science, 279, 2001, 398-403.

95. Bunjes, H., Effect of particle size on colloidal solid triglycerides, Langmuir, 16, 2000, 5234-5241.

96. Oyewumi, M. O., Mumper, R. J., Gadolinium-loaded nanoparticles engineering from microemulsion templates., Drug Development and Industrial Pharmacy, 28, 2002, 317-328.

97. Mehnert, W., Mader, K., Solid lipid nanoparticles, production, characterization and applications, Advanced Drug Delivery Reviews, 47, 2001, 165-196.

98. Hu, F.Q., Hong, Y.,Yuan, H., Preparation and characterization of solid lipid nanoparticles containing peptide, International Journal of Pharmaceutics, 273, 2004, 29-35.

99. Boltri, L., Canal, T., Esposito, P. A., Carli, F., Lipid nanoparticles: evaluation of some critical formulation parameters, Proceedings and program of the international symposium on controlled release of bioactive materials, 20, 1993, 346-347.

100. Tarimala, S., Dai, L. L., Structure of microparticles in solid-stabilised emulsions, Langmuir, 20, 2004, 3492-3494.

101. Miller, R., Fainerman, V. B., Kovalchuk, V. I., Grigoriev, D. O., Leser, M. E., Michel, M., Composite interfacial layers containing micro-size and nano-size particles, Advances in Colloid and Interface Science, 128, 2006, 17-26.

102. Northern technology testing (ntt) Cantel LTD-Royston Herts, UK. www.nttworldwide.com. Retrieved on 2008-11-05.

103. Macierzanka, A., Szelag, H., Microstuctural behaviour of water-in-oil emulsions stabilised by fatty acid esters of propylene glycol and zinc fatty acid salts, Colloids and Surfaces A: Physicochemical and Engineering Aspects, 281, 2006, 125-137.